Journal of proteome research

pubs.acs.org/jpr

Article

Incomplete Systemic Recovery and Metabolic Phenoreversion in Post-Acute-Phase Nonhospitalized COVID-19 Patients: Implications for Assessment of Post-Acute COVID-19 Syndrome

Elaine Holmes,* Julien Wist,* Reika Masuda, Samantha Lodge, Philipp Nitschke, Torben Kimhofer, Ruey Leng Loo, Sofina Begum, Berin Boughton, Rongchang Yang, Aude-Claire Morillon, Sung-Tong Chin, Drew Hall, Monique Ryan, Sze-How Bong, Melvin Gay, Dale W. Edgar, John C. Lindon, Toby Richards, Bu B. Yeap, Sven Pettersson, Manfred Spraul, Hartmut Schaefer, Nathan G. Lawler, Nicola Gray, Luke Whiley, and Jeremy K. Nicholson*

Cite This: *J. Proteome Res.* 2021, 20, 3315−3329

Read Online

ACCESS | Metrics & More | Article Recommendations | Supporting Information

ABSTRACT: We present a multivariate metabotyping approach to assess the functional recovery of nonhospitalized COVID-19 patients and the possible biochemical sequelae of "Post-Acute COVID-19 Syndrome", colloquially known as long-COVID. Blood samples were taken from patients ca. 3 months after acute COVID-19 infection with further assessment of symptoms at 6 months. Some 57% of the patients had one or more persistent symptoms including respiratory-related symptoms like cough, dyspnea, and rhinorrhea or other nonrespiratory symptoms including chronic fatigue, anosmia, myalgia, or joint pain. Plasma samples were quantitatively analyzed for lipoproteins, glycoproteins, amino acids, biogenic amines, and tryptophan pathway intermediates using Nuclear Magnetic Resonance (NMR) spectroscopy and mass spectrometry. Metabolic data for the follow-up patients (n = 27) were compared with controls (n = 41) and hospitalized severe acute respiratory syndrome SARS-CoV-2 positive patients (n = 18, with multiple time-points). Univariate and multivariate statistics revealed variable patterns of functional recovery with many patients exhibiting residual COVID-19 biomarker signatures. Several parameters were persistently perturbed, e.g., elevated taurine ($p = 3.6 \times 10^{-3}$ versus controls) and reduced glutamine/glutamate ratio ($p = 6.95 \times 10^{-8}$ versus controls), indicative of possible liver and muscle damage and a high energy demand linked to more generalized tissue repair or immune function. Some parameters showed near-complete normalization, e.g., the plasma apolipoprotein B100/A1 ratio was similar to that of healthy controls but significantly lower ($p = 4.2 \times 10^{-3}$) than post-acute COVID-19 patients, reflecting partial reversion of the metabolic phenotype (phenoreversion) toward the healthy metabolic state. Plasma neopterin was normalized in all follow-up patients, indicative of a reduction in the adaptive immune activity that has been previously detected in active SARS-CoV-2 infection. Other systemic inflammatory biomarkers such as GlycA and the kynurenine/tryptophan ratio remained elevated in some, but not all, patients. Correlation analysis, principal component analysis (PCA), and orthogonal-partial least-squares discriminant analysis (O-PLS-DA) showed that the follow-up patients were, as a group, metabolically distinct from controls and partially comapped with the acute-phase patients. Significant systematic metabolic differences between asymptomatic and symptomatic follow-up patients were also observed for multiple metabolites. The overall metabolic variance of the symptomatic patients was significantly greater than that of nonsymptomatic patients for multiple parameters (χ^2 p = 0.014). Thus, asymptomatic follow-up patients including those with post-acute COVID-19 Syndrome displayed a spectrum of multiple persistent biochemical pathophysiology, suggesting that the metabolic phenotyping approach may be deployed for multisystem functional assessment of individual post-acute COVID-19 patients.

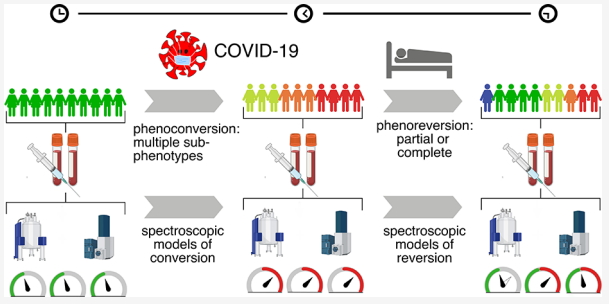

KEYWORDS: *COVID-19, post-acute COVID-19 syndrome, long-COVID syndrome, SARS-CoV-2, plasma, phenoconversion,*

continued...

Received: March 19, 2021
Published: May 19, 2021

Table 1. Summary of Reported Persistent COVID-19 Symptoms and Conditions from Multiple Studies

reported symptom, function, and/or condition	study type and (number of patients)	follow-up time	incidence and comments
lung function	cross-sectional, follow-up (238)	4 months	51.6% of patients showed reduced lung function[29]
	follow-up (58)	2−3 months	64% of patients experienced breathlessness; 60% showed lung abnormalities on MRI[4]
	follow-up (110)	8 weeks	44% of patients had persistent lesions as seen by the CT scan[30]
dyspnea	follow-up (938)	1.5−6 months	16% reported dyspnea[31]
	cross-sectional (2113)	mean 79 days	71% self-reported persistent dyspnea[3]
	cross-sectional (150 000)	2 months	43% self-reported dyspnea[32]
cardiac abnormalities	MRI (26)	1−2 months	19% of the participants in a study in athletes had cardiac abnormalities, mainly isolated myocardial edema[33]
	MRI (100)	64−92 days	ongoing myocardial inflammation in 60 patients (60%) without pre-existing heart conditions[8]
liver dysfunction	253 patients	2 months	increased liver enzymes, ALP and AST[9]
thyroid dysfunction	case report (1)	16 days	Graves' thyrotoxicosis in a female aged 21 years, following mild symptoms[34]
	case report (1)	7 weeks	subacute thyroiditis in a female aged 21 years, following mild COVID symptoms[35]
	case report (1)	toward the end of infection	thyroid dysfunction in a male aged 34 years[36]
hypokalemia	case study (1)	5 months	hypomagnesemia also noted[37]
anosmia/hyposmia/parosmia	retrospective questionnaire (117)	3−61 days	8.57% with persistent anosmia[38]
	multicenter patient recall, (111)	28−169 days	25% of the patients with anosmia/hyposmia during infection failed to recover[7]
	follow-up (938)	1.5−6 months	12% reported loss of smell; 10% loss of taste[31]
chronic fatigue	cross-sectional (1655)	175−199 days	63% reported fatigue and/or muscle weakness[17]
	cross-sectional (384)	54 days	69% reported fatigue, 30.1 and 9.5% had persistently elevated D-dimer and C-reactive protein, respectively[5]
	cross-sectional, follow-up study (238)	4 months	40.5% patients had low function on the 2 min walk test[29]
	cross-sectional (120)	6 months	17.5% persistent fatigue[39]
	cross-sectional (2113)	mean 79 days	87% self-reported persistent fatigue[3]
	cross-sectional 150 000	2 months	53% self-reported chronic fatigue[32]
diabetes	cross-sectional (734)	various	1.4% developed new-onset diabetes mellitus[40]
	systematic review (3711 cases)	various	492 diagnosed cases of new-onset diabetes across eight studies[41]
sleep difficulties	cross-sectional (1655)	175−199 days	26% with sleep difficulties[17]
hallucinations	case report (1)	3 months	female, 46 years old, presented with persistent auditory and visual hallucinations[42]
cognitive impairment	cross-sectional (18)	20−105 days	sustained mild cognitive deficits (78% patients) and lower testing performance[6]
unilateral facial nerve palsy	case study (1)	1 week	male, 37 years[43]
reactive arthritis	case study (1)		female, 39 years[44]
Guillain−Barré syndrome	case study (1)		male, recurring viral-related GBS episodes[45]
	case study (1)	53 days	male, 46 years, acute inflammatory demyelinating polyradiculoneuropathy[46]
skin conditions	cross-sectional (103)	>60 days	6.8% with persistent lesions[10]

phenoreversion, biomarkers, multiorgan disease, lipoproteins, amino acids, post-acute COVID-19 syndrome

INTRODUCTION

The COVID-19 pandemic continues, and although infection rates are currently reduced in many locations and multiple vaccines are now being deployed, the severe acute respiratory syndrome SARS-CoV-2 virus continues to evolve, yielding more infectious variants that are likely to maintain high infection rates. There is increasing concern about the alarmingly high number of patients not recovering from SARS-CoV-2 infections, resulting in "Post-Acute COVID-19 Syndrome (PACS)" with multiple persistent and highly variable symptoms (Table 1). A recent meta-analysis found that up to 80% of patients display one or more post-acute COVID-19 symptoms including fatigue (58%), headache (44%), attention disorder (27%), hair loss (25%), and dyspnea (24%), with joint pain (27%) and chest pain (22%) being among the most common postinfection symptoms.[1,2] Postinfection lung damage is a problem with several groups reporting 50% or more of patients with lung structure abnormalities and shortness of breath (dyspnea, up to 70% of patients),[3,4] long-term neurological complications including chronic fatigue (17.5−87% of patients[5]), cognitive impairment (up to 78%[6]), and anosmia/hyposmia (8.5−25%[7]) being reported, as well as cardiomyopathies or other structural cardiac abnormalities (up to 60%[8]); liver dysfunction;[9] disruption of the microvasculature; skin rashes[10] and discoloration and a range of autoimmune phenomena.[11] Diabetes has been proposed as a severity risk factor, but sadly, the considerable stress imposed on the body following the acute infection has resulted in new-onset diabetes mellitus in a number of patients.[12] Based on multiple

https://doi.org/10.1021/acs.jproteome.1c00224
J. Proteome Res. 2021, 20, 3315−3329

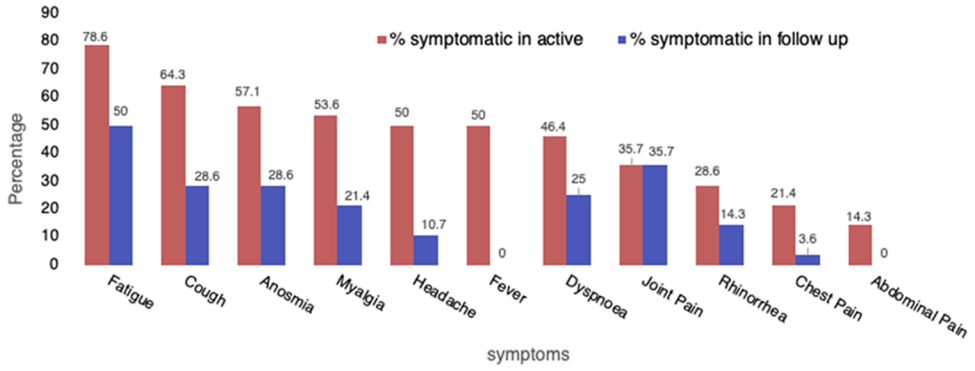

Figure 1. Comparison of percentage of the symptoms recorded at the time of acute illness in relation to the percentage recorded for the same patients at follow-up.

study observations including our own, the metabolic sequelae of SARS-CoV-2 infection are complex, engaging multiple-organ dysfunction presumed to be driven by immunopathological events including, for example, cytokine storms.[13,14] Related coronavirus diseases, Middle East respiratory syndrome (MERS) and SARS, have also been shown to induce long-term metabolic changes in recovered patients pertaining to hypertriglyceridemia, disorders of glucose metabolism, and liver function, further underlying the considerable need to support recovery and repair of the body during the post-COVID period.[15,16] The similarities between the SARS-CoV-1 and SARS-CoV-2 outbreaks also extend to the neurological consequences, with 54% of patients experiencing fatigue and 60% experiencing sleep disturbances 6 months post infection.[17] In some patients recovering from severe infection, residual postmedication treatment side effects have been reported: (i) hydroxychloroquine and cardiotoxicity; and (ii) long-term use of painkillers and renal and gastrointestinal dysfunction.[18] However, patients who suffered from less-severe manifestations of COVID-19 constitute the largest proportion of the active or post-acute COVID-19 population, now over 160 million worldwide, with few follow-up studies published to date. Within this mild-symptom COVID-19 group, hypometabolism in multiple brain regions[19] and persistent elevation of plasma D-dimer and C-reactive protein have been reported.[20] As is the case with most diseases, mildly affected patients are normally expected to show better functional recovery than seriously affected patients, but there is growing evidence that even mild cases can have persistent effects even a year post acute infection.[17,21] A recent comprehensive review of post-acute COVID-19 syndrome presents the key persistent manifestations of the disease and illustrates the enormous potential consequences in terms of global healthcare burden and individual suffering.[22]

Given the variability of clinical presentation and severity of the disease, recovery from COVID-19 is likely to be heterogeneous, in terms of both time to recovery and completeness of recovery. Severity of COVID-19 has so far been mainly classified in relation to respiratory symptoms in the acute stage, but the complex systemic symptoms require further consideration, with respect to both classifying the acute illness and assessing patient functional recovery. We and others have observed metabolic heterogeneity in the biomarker responses in acute COVID-19 patients showing multiple systemic effects.[23−28] We postulate that full functional recovery from the disease, by most of the patients without pre-existing comorbidities, is likely to be reflected in a normalization of the disrupted sentinel biomarker parameters and the overall metabolic phenotype. The process of multilevel recovery can be considered to be functionally equivalent to the reverse of disease onset and progression "phenoconversion",[23,24] during which the measured metabolic profile shifts from normality to one typical of the disease or its subphenotypes. From a theoretical point of view, patient "phenoreversion" therefore would be partial or complete, reflecting the degree of systemic recovery from COVID-19 infection. Going forward, this framework which employs sentinel biomarkers and appropriate multivariate models for mapping recovery from COVID-19 can be used to objectively assess other immunologically driven multisystem diseases.

The expected heterogeneity of the recovery responses for a complex system disease such as COVID-19 requires a nonstandard approach to understand and interpret the biochemical profiles of PACS individuals. There are precedents for metabolic modeling of single-organ or complex multiorgan damage and partial recovery in experimental toxicology studies where the onset, progression, and recovery or nonrecovery from toxicity can be followed using biofluid metabolic models.[47] Multiple studies using exemplar toxins that damage different organ systems in experimental animals at various times post dosing have been documented,[48−50] and some studies have shown sequential organ toxicity or recovery trajectories.[51,52] In such situations, functional biochemical recovery may occur at different rates and vary between individuals.[53] We hypothesize that because SARS-CoV-2 infections frequently result in multiorgan involvement the functional recovery of patients might show similar complex temporal patterns and variations in biochemical normalization through time and that study of these processes can provide an objective functional classification of recovery.

To assess the longer-term effects of COVID-19 infection in nonhospitalized patients, we obtained blood plasma samples at approximately 3 months following the acute phase of the disease and recorded persistent symptoms of patients at 6 months as well as their original symptoms during the acute phase of the disease. We adopted a targeted approach in which validated analytical methods were used to focus on metabolic parameters that had previously been described as biomarkers (Tables S1−S4) in the active phase of COVID-19.[23,26,54] This approach enables quantitative phenoreversion to be assessed and patients with incomplete functional recovery to be identified. We examined these variables from both univariate and multivariate modeling perspectives to investigate individual and group recovery behaviors. The data were evaluated with respect to a range of terms of possible phenoreversion outcomes. The

https://doi.org/10.1021/acs.jproteome.1c00224
J. Proteome Res. 2021, 20, 3315−3329

principal aim of this study was to develop the basis of an objective metabolic framework for measuring systemic recovery in COVID-19 patients using a range of metabolic technologies and biomarkers.

METHODS

Participants and Reported Symptoms at Follow-Up

Three cohorts were examined: (i) a healthy control group (n = 41); (ii) a hospitalized patient group (n = 18 with multiple time-points) sampled during the acute infection phase; and (iii) a recovery cohort consisting of a nonhospitalized group sampled 3 months post the acute phase of the disease (n = 27) with acute-phase symptoms and symptoms 6 months post COVID infection. The participant demographics and the numbers of patients and samples used for each assay are provided in Tables S5 and S6. From the recovery cohort, 57% of the participants recorded one or more persistent symptoms, with the majority having more than one symptom. A graphical description of the follow-up symptomatic patients in relation to the acute-phase symptoms is shown in Figure 1. In addition to persistent respiratory symptoms including cough, dyspnea, and rhinorrhea, there were also nonrespiratory "systemic" symptoms including fatigue, anosmia, myalgia, and joint pain, which are indicative of wider systematic damage and inflammatory components, highlighting the systemic nature of post-acute COVID-19 syndrome. Many of these longer-term symptoms have been reported in previous studies as itemized in Table 1, suggesting that this group is similar to other follow-up populations, bearing in mind that in the current case these were previously nonhospitalized patients. Note, however, that with the exception of anosmia, many of these symptoms are common to aging populations, and without an accurate framework of assessment, we cannot be entirely certain of the direct association of these symptoms with PACS. On balance, the fact that these symptoms were measured in the same participants during and post infection should partially standardize the collection of metadata. Thus, we aimed to develop an independent metric of PACS and recovery that does not rely purely on reported symptoms.

^{1}H NMR Spectroscopy of Blood Plasma

^{1}H NMR spectroscopy was completed according to a previously published method[55] briefly described as follows: blood was centrifuged at 13 000g for 10 min at 4 °C and the plasma supernatant was mixed with buffer (75 mM Na_2HPO_4, 2 mM NaN_3, 4.6 mM sodium trimethylsilyl propionate-[2,2,3,3-$^2H_4$] (TSP) in 80% D_2O, pH 7.4 ± 0.1) (1:1); 600 μL of each plasma/buffer mixture was transferred into a Bruker SampleJet NMR tube (5 mm) and sealed with POM balls added to the caps. For quality control samples, long-term reference samples were used, prepared using the same methods as for the study samples. A validated sampling preparation and handling protocol for COVID-19 samples was used as previously described.[56]

NMR measurements were performed on one of two Bruker 600 MHz Avance III HD spectrometers (in vitro diagnostics research (IVDr)) equipped with a BBI probe and fitted with Bruker SampleJet robots with the cooling system set to 5 °C. A quantitative calibration was completed prior to the analysis using the protocol of Dona et al.[55] All experiments were completed using the Bruker in vitro diagnostics research (IVDr) methods.[57] For each sample, three experiments were completed in automation with a total analysis time of 12.5 min: a ^{1}H one-dimensional (1D) experiment with solvent presaturation (32 scans, 98 304 data points, spectral width of 18 028.85 Hz), a Carr−Purcell−Meiboom−Gill (CPMG) spin-echo experiment (32 scans, 73 728 data points, spectral width of 12 019.23 Hz), and a two-dimensional (2D) J-resolved experiment (two scans with 40 t_1 increments). All data were processed in automation using Bruker Topspin 3.6.2 and ICON NMR to achieve phasing, baseline correction, and calibration to TSP (δ = 0). On completion of the run, the samples were transferred directly to the second NMR spectrometer and DIffusional and Relaxation Editing (DIRE) spectra were obtained (64 scans, 98 304 data points, spectral width of 18 028.85 Hz).[54]

Lipoprotein reports itemizing 112 lipoprotein parameters for each plasma sample were generated using the Bruker IVDr Lipoprotein Subclass Analysis (B.I.LISA) method.[57] This was completed by quantifying the $-CH_2$ (δ = 1.25) and $-CH_3$ (δ = 0.8) peaks of the 1D spectrum after normalization to the Bruker QuantRef manager within Topspin using a PLS-2 regression model. The lipoprotein subclasses included different molecular components of very low-density lipoprotein (VLDL, 0.950−1.006 kg/L), low-density lipoprotein (LDL, density 1.09−1.63 kg/L), intermediate-density lipoprotein (IDL, density 1.006−1.019 kg/L), and high-density lipoprotein (HDL, density 1.063−1.210 kg/L). The LDL subfraction was further divided into six density classes (LDL-1 1.019−1.031 kg/L, LDL-2 1.031−1.034 kg/L, LDL-3 1.034−1.037 kg/L, LDL-4 1.037−1.040 kg/L, LDL-5 1.040−1.044 kg/L, and LDL-6 1.044−1.063 kg/L), and the HDL subfractions were divided into four different density classes (HDL-1 1.063−1.100 kg/L, HDL-2 1.100−1.125 kg/L, HDL-3 1.125−1.175 kg/L, and HDL-4 1.175−1.210 kg/L).

The α-1-acid glycoprotein N-acetyl-glucosamino (N-acetyl) signal integrals were calculated as GlycA from the superimposition of terminal N-acetyl signals (δ 2.03) and GlycB was calculated from branched-chain N-acetyl signals (δ 2.07) determined by the DIRE spectra. The supramolecular phospholipid composite (SPC_{total}) signals (δ = 3.20−3.30) were determined from the DIRE spectra by integration, a method previously described and applied to COVID-19 studies.[54] The SPC_{total} parameter consists of the $N^+-(CH_3)_3$ choline headgroup signals of lysophosphatidylcholines carried out on plasma glycoproteins and from phospholipids in high-density lipoprotein subfractions together with a phospholipid component of LDL.

Mass Spectrometry (MS) and Amino Acid/Biogenic Amine Quantification

Fully quantitative amino acid analysis of 35 molecular species was performed using an ultra-high-performance liquid chromatography (UHPLC)-quadrupole time-of-flight (QToF)-based MS method following derivatization.[58] Amino acid standards and ammonium acetate were purchased from Sigma-Aldrich (MO). Stable-isotope-labeled (SIL) internal standard non-canonical and canonical amino acid mixes were purchased from Cambridge Isotope Laboratories (MA). Water, acetonitrile, methanol, and isopropanol were all Optima-grade (from Thermo Fisher Scientific). Calibrators and quality controls were prepared from a standard solution of physiological amino acids (acids, basics, and neutrals) at 500 μM. Asparagine and glutamine were prepared freshly at 0.5 mM on the day of analysis due to their solution instability. A working aqueous stock solution of all amino acids was prepared at 400 μM and separately diluted to 200, 100, 40, 20, 10, 4, 2, and 1 μM for calibrators and to 300, 75, 15, and 3 μM for analytical quality

https://doi.org/10.1021/acs.jproteome.1c00224
J. Proteome Res. 2021, 20, 3315−3329

controls. A stable-isotope-labeled (SIL) internal standard solution (12.5 μM in water) was prepared from stocks of canonical and noncanonical amino acids at 2.5 mM in water and stored at −20 °C until use. Following the addition of the SIL working solution to each sample, methanol was added to effect protein precipitation. Following centrifugation, the extract supernatant was taken for a derivatization step with the AccQTag reagent (Waters Corp., Milford, MA). Samples were finally diluted 1:50 with liquid chromatography (LC)-MS-grade water for LC-MS analysis.

Liquid Chromatography-Mass Spectrometry

Amino acid analysis was performed using a Waters Acquity I-class UPLC system (Waters Corp., Milford, MA) coupled to a Bruker impact II QToF mass analyzer (Bruker, Daltonics, Billerica, MA). Chromatographic separation was achieved using an Acquity UPLC HSS T3 1.8 μm 2.1 × 150 mm^2 column (Waters, Milford, MA). Eluent A consisted of 2 mM ammonium acetate in water, and eluent B consisted of 2 mM ammonium acetate in acetonitrile/water 95/5 (v/v). The flow rate was 0.6 mL/min, and the column temperature was maintained at 45 °C. The autosampler compartment was cooled to 4 °C, and a 2 μL injection volume was performed using the full-loop injection mode. Gradient elution was performed starting with 5% B for 0.2 min, increasing to 30% B at 5 min and 100% B at 5.1 min for 1 min before returning to 5% B until 7.5 min. The weak and strong washes were water/acetonitrile 95/5 (v/v) and isopropanol, respectively. The mass analyzer was operated with positive electrospray ionization (ESI) in the broadband collision-induced dissociation (bbCID) mode, enabling MS and tandem mass spectrometry (MS/MS) spectral data collection within the same run. The ion source settings were as follows: capillary voltage = 4.5 kV; end plate offset = 500 V; drying gas flow = 12.0 L/min; nebulizer gas = 5.0 bar; drying temperature = 250 °C. The data acquisition rate was set to 8 Hz over the mass range of m/z 30−1000. The collision energy for the MS scan was set to 6.0 eV, and alternating low and high energies for MS/MS were set at 20 and 50 eV. An internal calibration was performed by injection of 5 mM aqueous sodium formate/isopropanol (50:50 v/v) at the beginning of every run. Mass spectrometric data were collected with Compass HyStar 5.1 and O-TOF Control version 5.2. MS data were processed using TASQ 2.2 (Bruker Daltonics, Bremen, Germany). The molecular formula or exact mass of the derivatized amino acid was used to extract the precursor ions with a mass error of <3 mDa. Calibration curves were linearly fitted with a weighting factor of $1/x$.

Tryptophan Pathway Metabolite Quantification

Quantitative analysis of tryptophan and 14 catabolites in its metabolic pathway was performed as previously reported.[26,59] Analysis was performed on 50 μL of plasma, with the addition of SIL prior to protein precipitation with methanol containing 2 mM ammonium formate. After mixing, samples were transferred to a Phenomenex PHREETM phospholipid removal solid-phase extraction plate (Phenomenex, NSW, Australia). PHREE plates were washed with methanol containing 2 mM ammonium formate, and the eluent was dried using a SpeedVac vacuum concentrator (Thermo Fisher, MA). Extracts were resuspended in 100 μL of aqueous 0.1% formic acid prior to LC-MS analysis.

Liquid Chromatography-Mass Spectrometry

LC-MS analysis was performed on a Waters Acquity UPLC (Waters Corp., Milford, MA) coupled to a Waters Xevo TQ-XS MS (Waters Corp., Wilmslow, U.K.). Separation was performed on a Waters HSS T3 1.8 μm, 2.1 × 150 mm^2 column maintained at 45 °C. Linear gradient elution was performed at 0.6 mL/min. The mobile phase was composed of 0.1% formic acid in 2 mM ammonium formate (v/v) (A) and 0.1% formic acid in acetonitrile (v/v) (B), starting at 1% B, increasing to 10% B over 3 min, and then increasing to 90% B at 4 min, and finally returning to 1% B at 4.1 min for column re-equilibration, which was completed at 5 min. The weak and strong washes were 95:5 water/acetonitrile (v/v) and 100% isopropanol, respectively. Mass spectrometric data were collected with MassLynx version 4.2 and processed using the TargetLynx package (Waters Corp., Milford, MA).

Parameter Selection

Following a standard suite of NMR and targeted MS assays, 34 biogenic amines[59] and 15 tryptophan pathway parameters[60] were measured by mass spectrometry and 112 lipoprotein parameters, and glucose,[23] plus glycoproteins, and novel supramolecular phospholipid composite biomarkers previously identified and measured by NMR spectroscopy.[54] In addition, we calculated multiple ratios. Based on modeling these data in relation to SARS-CoV-2 positivity, we selected 45 discriminatory primary parameter measurements and 7 ratios (see Tables S1−S4) to evaluate the extent or recovery of the nonhospitalized patients in relation to the SARS-CoV-2 positive and the healthy control groups.

Spectroscopic Data Modeling

NMR and MS-derived data were combined and interrogated using principal component analysis (PCA) and orthogonal-partial least-squares discriminant analysis (O-PLS-DA) as unsupervised and supervised multivariate analysis techniques, respectively.[61] Data were mean-centered and autoscaled prior to multivariate modeling. Both PCA and O-PLS-DA analysis tasks were performed in the statistical programming language R, using the metabom8 package (v0.4.2), obtainable at https://github.com/tkimhofer. See also the Supporting Information.

O-PLS-DA Modeling

The sample set for both the targeted assays (28 healthy controls and 26 follow-up SARS-CoV-2 participants) and the lipoproteins (40 healthy controls and 27 follow-up) comprised a single time point from the healthy controls and the follow-up patients. An O-PLS model with one orthogonal + one predictive component each was established, and the optimal number of components was determined using the area under the receiver operator characteristic curve (AUROC) determined with the predictive component scores calculated in an internal Monte Carlo cross-validation (CV) procedure ($AUROC_{CV}$ = 0.86, R^2X = 0.16 for the targeted MS data; $AUROC_{CV}$ = 0.81, R^2X = 0.29 for lipoprotein data).

RESULTS AND DISCUSSION

Based on a selected subset of parameters that have been shown to be significantly perturbed in the active COVID-19 cases,[23,26] we estimated the functional recovery of individuals and the 3 month follow-up cohort as a whole. The full parameters sets were evaluated are shown in Tables S1−S4.

Evaluation of Univariate Parameters in Healthy, Acute, and Follow-Up Patients

For many of the metabolic and lipoprotein parameters characteristically altered during SARS-CoV-2 infection, a normalization to concentrations within the healthy range occurred. Other parameters remained elevated or depleted, or

https://doi.org/10.1021/acs.jproteome.1c00224
J. Proteome Res. 2021, 20, 3315−3329

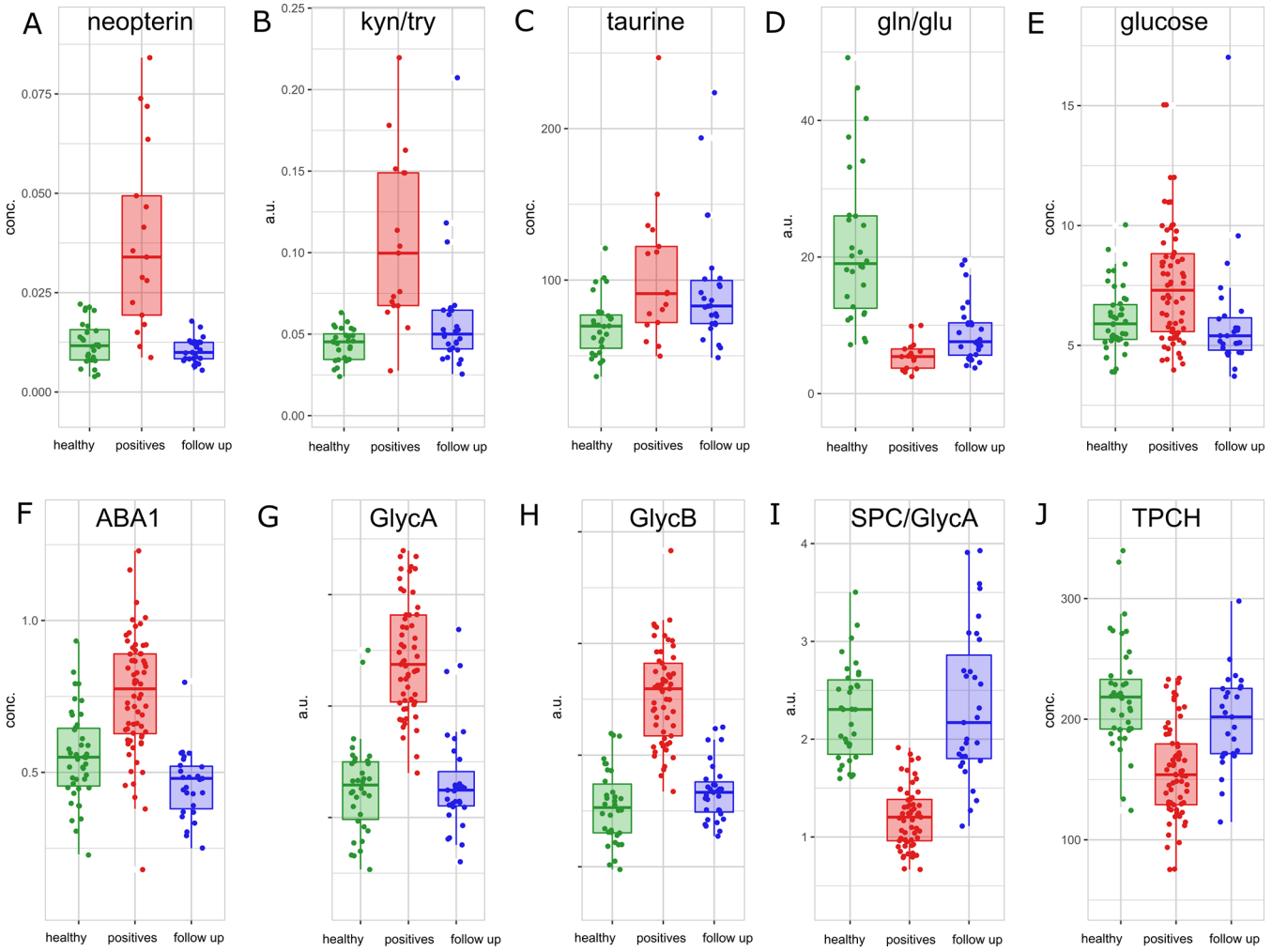

Figure 2. Ten exemplar univariate plasma metabolic parameters in healthy, SARS-CoV-2-positive, and follow-up patients showing a range of individual and group phenoreversion and nonrecovery patterns. (A) Neopterin, (B) kynurenine/tryptophan ratio, (C) taurine, (D) glutamine/glutamate ratio, (E) glucose, (F) lipoprotein ABA1 fraction, (G) glycoprotein A integral, (H) glycoprotein B integral, (I) SPC_{total}/glycoprotein A ratio, and (J) lipoprotein total plasma cholesterol (TPCH).

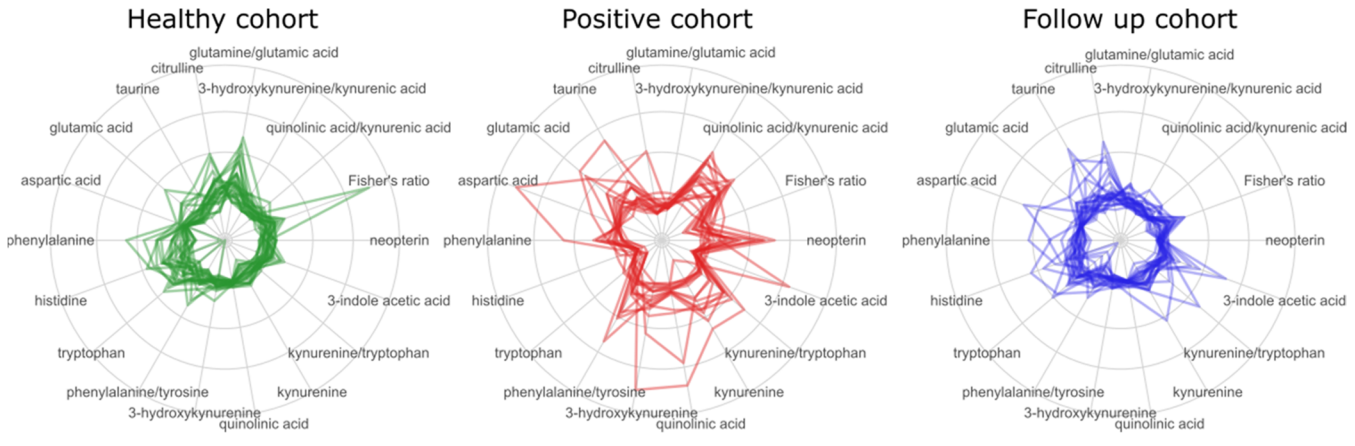

Figure 3. Radar plots of amino acid and biogenic amine data, standardized and displayed separately for each cohort. Each individual is shown as a connected ring of metabolite concentrations.

showed a partial normalization. A series of 10 exemplar univariate metabolic parameter comparisons between plasma samples from healthy, SARS-CoV-2 positive, and post-acute COVID-19 patients is shown in Figure 2. In addition to these examples of "normalized/non-normalized" behavior, equivalent data for all 52 parameters are provided in Figures S1−S18, S22−S50, and S54−S58. In Figure 2A, we show examples of parameters that reverted to baseline level including neopterin, glucose, ABA1 in contrast to parameters that remained at levels more typical of acute SARS-CoV-2 infection than healthy, i.e.,

https://doi.org/10.1021/acs.jproteome.1c00224
J. Proteome Res. 2021, 20, 3315−3329

substantially not normalized, such as taurine in the follow-up patients, which was significantly different to healthy controls (Mann−Whitney test $p = 3.6 \times 10^{-3}$) and the glutamine-to-glutamate ratio also significantly different to control (Mann−Whitney test, $p = 6.95 \times 10^{-8}$). For several parameters, the majority of the participants had normalized with serum concentrations falling within the range for healthy participants but leaving a small subset of participants with concentrations or ratios in the same range as the active disease COVID-19 patient group. Parameters that were substantially normalized included GlycA, GlycB, total plasma cholesterol (TPCH), and the kynurenine/tryptophan and SPC/GlycA signal ratios, but in all cases, there were patient outliers that had not normalized underscoring the heterogeneity of response to SARS-CoV-2 infection. The HDL parameters H4A1, H4A2 (apolipoproteins A1 and A2 in HDL subfraction 4), and kynurenine were partially normalized, and the mean of the follow-up cohort lay between the means of the healthy and the SARS-CoV-2-infected groups with approximately equal numbers of participants with values in the range for the healthy and infected (Figures S10, S30, and S31).

The radar plots for individual patients and participants (Figure 3) clearly show that the SARS-CoV-2 group is defined by elevated plasma levels of tryptophan pathway metabolites. Plasma neopterin levels were markedly elevated in active-phase COVID-19 infections as previously reported,[23,62] but the follow-up patients were essentially at control neopterin levels in this cohort. Neopterin is generated in macrophages and microglia under the influence of the tumor necrosis factor (TNF)-α and γ-interferon[62] and is a marker of early-stage cell-mediated acute inflammation and as such would be expected to recover soon after the acute inflammatory phase.[63] A similar pattern in neopterin levels was observed following infection with SARS-CoV-1, where neopterin levels were directly associated with fever.[64] Further insights come from inspection of the "radar" parameter plots for individuals in each group where each individual is connected across all their measured parameters as shown in Figure 3. There are notable differences in the individual shapes for the groups with biomarker pointers in each set. Interestingly, plasma concentrations of 3-indole acetic acid were higher in the recovery cohort 3 months after infection than in the infected or healthy groups (Figures 3 and S9), suggestive of a gut microbiome functional change. Indoles are known to activate the aryl-hydrocarbon-receptor (AhR), a ligand-activated transcription factor that has been shown to reduce inflammation and stimulate metabolic circuits by integrating signals from the host, the microbes, and dietary intake.[65] Additional microbe indole-derived metabolites are, for example, indole-3-acetylaldehyde and indole-3-aldehyde, both known to reduce inflammation via AhR signaling in the intestine and the liver as well as to strengthen barrier function in the intestine.[66]

Several other metabolites behave in an analogous fashion with near-complete recovery for all patients (Tables S1−S4). For example, the kynurenine/tryptophan ratio (Figure 2B) is also substantially within the normal range for most patients 3 months post infection, with the exception of three individuals, who must be assumed to be still in a heightened inflammatory state. This is consistent with data showing acute systemic inflammatory activity during SARS-CoV-2 infection.[23,26,67,68] The ratio of tryptophan to kynurenine is predominantly mediated by indoleamine 2,3-dioxygenase activity and is generally associated with inflammation as well as immunomodulation in both infectious diseases and chronic inflammatory conditions, including neurological diseases such as Parkinson's disease,[69] diabetes,[70] and several autoimmune conditions such as rheumatoid arthritis,[71] systemic lupus erythematosus,[72] and primary sclerosing cholangitis.[73]

Plasma taurine concentrations were also increased in the acute phase of COVID-19[23] but also appear substantially elevated in the 3 month follow-up patients with respect to controls (Figure 2C). Elevated taurine levels have previously been associated with liver injury and hepatotoxicity in man and experimental animals,[74] but high levels of taurine are also present in large quantities in cardiac and skeletal muscles[75,76] and muscle damage has been associated with taurinaemia as a measure of tissue damage.[77] As COVID-19 causes considerable skeletal muscle mass loss,[78] it is possible that high plasma taurine may simply reflect muscle turnover. We noted that Fischer's ratio, a marker of liver injury, was substantially normalized for most follow-up patients (Figure S5). However, persistent liver dysfunction with elevated ALT and AST has also been noted post COVID-19 in other studies (Table 1). The relative sensitivity for Fischer's ratio versus plasma taurine versus serum transaminases as markers of liver injury severity has not been evaluated to our knowledge. Macroscopic cardiac damage is also a known persistent consequence of acute SARS-CoV-2 infection (Table 1), and it is possible that high plasma taurine is reflective of longer-term multiple-organ damage including the liver, heart, and skeletal muscle components, but this remains speculative. Given that the nonhospitalized patients studied here were relatively mildly affected in the acute phase, these observations are a cause for concern and warrant a larger-scale study of the persistence of elevated plasma taurine in COVID-19 patients and its clinical significance.

Acute-phase COVID-19 patients show elevated plasma glutamate (Figure S6) and reduced glutamine levels[23,26,79] and a low glutamine/glutamate ratio, which is also substantially higher in the 3 month follow-up patients (Figure 2D). This ratio is driven both by elevated plasma glutamate relative to controls (Mann−Whitney test $p = 1.04 \times 10^{-3}$ versus controls, Figure S6) and by reduced plasma glutamine relative to controls (Mann−Whitney test $p = 7.00 \times 10^{-5}$). Glutamate is an important anaplerotic carbon source to the citric acid cycle[80] and thus plays major important cellular energy generation roles in multiple organs including the kidney, heart, and brain. Both renal and neurological effects of COVID-19 are now well-documented in the acute phase,[81] and again these data pose questions about the possible role of these metabolites in COVID-related organ dysfunction. Furthermore, glutamate is the major excitatory amino acid in the central nervous system (CNS) and elevated CNS levels can induce acute injury,[82] with the possible significance of this observation being amplified by knowledge that tryptophan metabolites 3-hydroxykynurenine and quinolinic acid are elevated in SARS-CoV-2 infections[23,26] and both are also excitatory neurotoxins.[83] Quinolinate and kynurenate (elevated in most acute COVID-19 patients) also modulate glutamate function, with increased plasma quinolinate resulting in cellular release of glutamate.[84] However, quinolinic acid levels are mainly normalized in the follow-up patients so they cannot be directly driving the glutamine/glutamate ratio. The relationship between glutamate and glutamine is important in immune cell homeostasis, especially T-cells and astrocytes within the CNS,[85] where it acts as an immunomodulator upregulating surface glutamate receptors on activation, and the rate of immune cell glutamine consumption increased in catabolic conditions including sepsis in which plasma glutamine

https://doi.org/10.1021/acs.jproteome.1c00224
J. Proteome Res. 2021, 20, 3315−3329

Figure 4. Spearman's correlation analysis from 1 (red) to −1 (blue) of plasma metabolic sentinel markers of COVID-19 (size of the dots is also equal to the correlation value). Hierarchical clustering analysis (HCA) was performed on the healthy correlation matrix to cluster variables exhibiting similar patterns, and the resulting order was applied to positive and follow-up COVID-19 patients for direct motif comparison.

levels may also be low.[86] So although the mechanistic significance of a low glutamine/glutamate ratio is not yet understood for COVID-19, the persistence of a significantly reduced ratio in the majority of the follow-up patients implies continuing post-COVID immunometabolic dysregulation.

Diabetes is a known risk factor for early progression to severe COVID-19 disease,[87] and new-onset diabetes has also been reported in COVID-19 patients.[41] Plasma glucose, a well-known marker of type 2 diabetes, was elevated in active-phase patients (Figure 2E), and high blood glucose on hospital admission has been associated with poor prognosis.[88] The 3 month follow-up patients appear to have a glucose distribution similar to that of the control patients (none of whom were diabetic) although there were several elevated plasma glucose outliers in both groups. Our tentative inference from these data is that diabetes does not appear to be a major persistent effect of SARS-CoV-2 infection in this nonhospitalized patient cohort. However, this statement cannot be generalized to cover other COVID-19 patient severity classes because the data set is relatively small and the patients were not hospitalized. Further studies on COVID-19 follow-up patients are required to evaluate the persistence of diabetes in patients who were more severely affected during the acute stage of the disease.

Lipoprotein dysregulation is a notable feature of acute COVID-19 disease.[24,89,90] The NMR spectroscopy-derived apolipoprotein B100/A1 ratios for the three groups are shown in Figure 2F. We have previously reported elevations in this ratio in COVID-19 patients, as have others.[24,27] The clinical significance of this ratio is that it is generally predictive of long-term atherosclerosis and coronary artery disease[91] and has previously been associated with a range of other cardiometabolic diseases.[92] All of the follow-up patients (except one) appear to be at the control level for this parameter. Other lipoprotein parameters apolipoproteins A1 and A2 were also normalized, respectively, and mostly normalized (Figures S47 and S48) although their exact relationships varied according to the degree of persistent symptoms (see below). The NMR-derived inflammatory markers GlycA and GlycB and the SPC/GlycA ratio were measured from the diffusion and relaxation-edited NMR spectra and are markedly altered in acute COVID-19 patients.[54] The GlycA and GlycB signals from acute-phase reactive proteins (mainly from α-1-acid glycoprotein but with contributions from other glycoproteins)[93] are strongly elevated in the active phase of COVID-19 and several follow-up patients still had elevated levels (Figure 2G,H). The SPC/Glyc ratio was reduced in active disease, and likewise, several follow-up patients had reduced ratios (Figure 2I). The SPC peak is a supramolecular cluster with several lysophosphatidylcholines and choline species being present bound to HDL and LDL and the α-1-acid glycoprotein.[54] This provides a metric for detection and discrimination of SARS-CoV-2 positivity and would appear to provide a potential measure of recovery from the COVID-19-related immunopathology. A reduction in plasma HDL cholesterol has been shown to be associated with COVID-19 infection.[23,24] The majority of patients showed normal total plasma cholesterol after 3 months, with one or two outliers that were still significantly reduced (Figure 2J).

Cohort-Level Variation in Metabolic Phenotypes

The patient signatures and variations of individual metabolic parameters in the COVID-19 follow-up patients shown in Figure 2 do not demonstrate the full system complexities of the metabolic interactions in the acute patient group. Differences

https://doi.org/10.1021/acs.jproteome.1c00224
J. Proteome Res. 2021, 20, 3315−3329

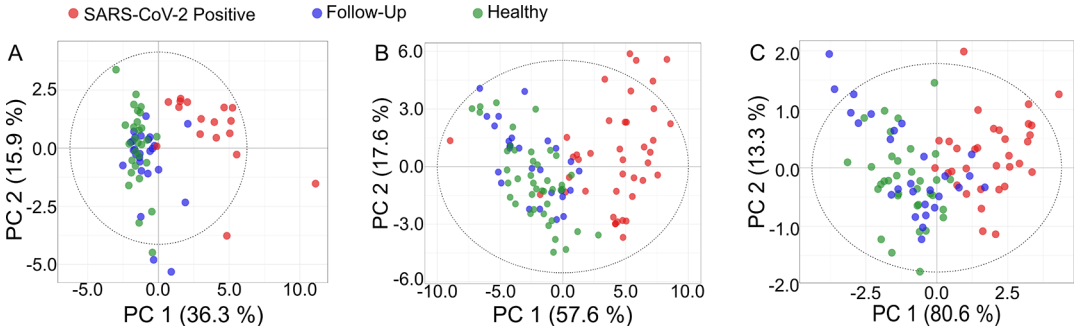

Figure 5. Principal component scores plots of the three cohorts probed by (A) targeted MS data, (B) IVDr lipoprotein data, and (C) the NMR-DIRE experiment extracted features, GlycA, GlycB, SPC_{total}, and the SPC/GlycA ratio. Limitations in available sample volumes for the different assays led to small differences in the sample numbers between the assays. In (A), there were 17 SARS-CoV-2 positive samples (red), 27 follow-up samples (blue), and 28 healthy control samples (green) in the targeted MS analysis (PC1 = 36.3%, PC2 = 15.9%). In (B), there were 40 SARS-CoV-2-positive samples (red), 27 follow-up samples (blue), and 40 healthy control samples (green) in the lipoprotein samples (PC1 = 57.6%, PC2 = 17.6%). In (C), there were 33 SARS-CoV-2-positive samples (red), 27 follow-up samples (blue), and 34 healthy control samples (green) in the DIRE-NMR extracted parameters (PC1 = 80.6%, PC2 = 13.3%). The multivariate confidence intervals (Hotelling's T, $\alpha = 0.95$) are shown as ellipses.

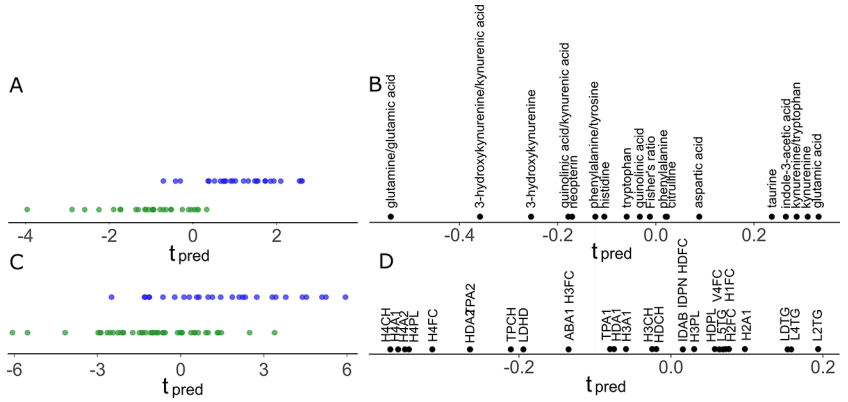

Figure 6. O-PLS-DA model plots of the predictive components for targeted MS analysis (A, B) and targeted lipoproteins (C, D) with selected variables. Blue dots on the O-PLS scores refer to the follow-up patients, and green dots refer to the healthy controls. (A) O-PLS scores of the targeted MS data with 28 healthy controls and 26 follow-up patient data. (B) OPLS loadings of (A) with 18 selected targeted assays and its ratio. (C) O-PLS scores of the targeted NMR-determined lipoproteins with 40 healthy controls and 27 follow-up patient data. (D) O-PLS loadings of (C) with 29 selected lipoproteins.

between group behaviors can be investigated by considering the correlation matrix structures of individual sentinel marker data as shown in Figure 4A (left) (healthy versus COVID-19 acute phase) and Figure 4B (right) (follow up versus healthy patients). The asymmetry of the paired matrices observed across the diagonals is an indicator of the systemic differences in metabolic relationships within the groups. Thus, if full functional recovery had occurred in the follow-up patients, the two correlation matrices would be substantially equivalent and, therefore, symmetrical. This is clearly not the case, and so as a group across multiple variables, the follow-up patients were not fully metabolically recovered. The glutamine/glutamate relationships, the liver-related plasma metabolic biomarkers (elevated taurine and low citrulline), and the tryptophan−kynurenine pathway intermediates (high quinolinic acid, kynurenine, 3-hydroxykynurenine) were also noticeably different in the three groups as indicated in the earlier univariate data.

Multivariate Statistical Analysis

To investigate further the multivariate metabolic relationships in the patient groups, we performed principal component analysis (PCA) using three different composite windows on metabolism involving amino acids and tryptophan targeted assays, lipoproteins (targeted), and concentrations of GlycA, GlycB, and SPC and the ratio GlycA/SPC estimated by integrating DIRE spectra, as previously described[54] (Figure 5A−C). Each metabolic window reveals different degrees of variable recovery because they cover different features of the systemic disease. PCA is primarily used here as a simple visualization tool to view group clustering behavior among SARS-CoV-2-positive (red), follow-up (blue), and healthy (green) patients and thus cannot be used in a diagnostic sense, merely as another indicator of general recovery. Figure 5A shows that most follow-up patients were substantially normalized with respect to their overall amino acid profiles with just a few outliers. However, PCA plots do not show all of the variance in the data set and are a crude clustering tool to visualize complex and heterogeneous sets. Lipoprotein data from the same patient samples also show substantial normalization in most patients but with multiple patients at or near the interface between the acute and healthy groups (Figure 5B). This is consistent with the intermediate nature of the correlation matrices shown in Figure 3. The extracted diagnostic features from the DIRE-NMR spectra from the same samples are shown in Figure 5C, with follow-up patient data points being scattered across the healthy and acute metabolic space. We have shown previously that the GlycA, GlycB, SPC, and SPC/Glyc ratios are highly diagnostic for SARS-CoV-2-positive versus controls and SARS-CoV-2 negative respiratory patients. These

https://doi.org/10.1021/acs.jproteome.1c00224
J. Proteome Res. 2021, 20, 3315−3329

are from acute-phase reactive glycoproteins, mainly α-1-acid glycoprotein (GlycA and B peaks) and the supramolecular phospholipid composite (SPC_{total}) peak from phospholipids bound to glycoproteins or HDL and LDL subfractions that reflect underlying immunopathological processes.[54] Thus, Figure 5C also illustrates the incomplete immunometabolic phenoreversion of a subset of follow-up patients as revealed by the SPC/GlycA inflammatory markers.

Having demonstrated the differential clustering behavior by PCA, we applied O-PLS-DA to determine the predictive components that separated the healthy from the follow-up participants with respect to both targeted MS data (Figure 6A,B) and lipoproteins (Figure 6C,D). The metabolic properties that distinguished these groups were mainly similar to the properties that have been reported previously as separating healthy from positive active-phase patients with higher glutamic acid, lower glutamine/glutamate ratios, higher kynurenine/tryptophan ratios, higher LDL parameters, and lower HDL parameters. Thus, a residual multivariate signature of the disease was still present at three months after the acute phase. In addition, indole-3-acetic acid also marked a difference present in the follow-up patients but was not a strong biomarker of the acute-phase disease,[23,26] as illustrated in the radar plot shown in Figure 3.

Modeling Metabolic Heterogeneity in Follow-Up Patients in Relation to the Presence or Absence of Persistent Symptoms

Examination of univariate plots of individual parameters revealed marked differences between the statistical distributions of data for follow-up patients who were symptom-free or symptomatic (for any clinical parameter) at 6 months. In particular, the observed variance in the symptomatic patient data appeared generally greater, suggesting a greater heterogeneity of biochemical states in patients with persistent symptoms. To assess this quantitatively, we performed a series of *F*-tests on the variances between the parameters of asymptomatic and symptomatic patients, two of which reached absolute statistical significance, viz. H3FC (Figure S28), free cholesterol in HDL fraction 3, $p = 0.027$; and TPCH (Figure S49), total plasma cholesterol, $p = 0.017$. However, we observed that, taken as a group, in the majority of cases, the lipoproteins' parameter variance was still greater for symptomatic than asymptomatic patients to a degree that seemed unlikely by chance alone. We confirmed this by applying a χ^2 test to these data, which gave a value of $p = 0.014$. This indicates that collectively the parameter variances were indeed significantly different between symptomatic and asymptomatic patients. This is not a predictive model, and although there are indications that follow-up metabolic profiles carry data that are potentially predictive of long-term symptomatic outcomes, this needs to be explored in larger patient data sets.

Further studies are required to evaluate the detailed long-term metabolic consequences of patients who suffered more significant acute effects and required interventions such as oxygen therapy and assisted ventilation than in the current nonhospitalized group where long-term effects might be less severe. There are several literature reports of multiple clinical symptoms in COVID-19 patients extending 6 months to a year beyond hospitalization,[17] and serious accompanying metabolic abnormalities would be unsurprising. Long-term metabolic effects of SARS-CoV-1 have been reported up to 12 years post the critical illness phase; these included liver dysfunction and hypertrigylceridemia,[94] and it is a possibility that COVID-19 will create similar long-term outcomes. The original SARS-CoV-1 virus affected 8098 patients worldwide;[95] given that the COVID-19 pandemic has now affected over 141 million people, if disability were then scaled to the same level as seen with SARS, such long-term effects would represent a major increase in global healthcare burdens and associated healthcare costs. Thus, it is imperative to implement large-scale follow-up studies to assess PACS healthcare liabilities in each population and also to understand the long-term immunopathological drivers or disease and to help identify patients with post-acute COVID-19-syndrome healthcare needs to mitigate any persistent disorders and optimize patient recovery.

SUMMARY AND CONCLUSIONS

Metabolic phenotyping appears to be a highly effective tool for assessing phenoreversion and functional systemic recovery of patients following COVID-19 and the evaluation of post-acute COVID-19 syndrome. There are clear metabolic patterns associated with persistent inflammatory and metabolic derangements in a majority of nonhospitalized 3-month-post-COVID-19 patients, with one or more symptoms being persistent in 57% up to 6 months following the acute phase. Most metabolic parameters showed a high level of normalization. Other biomarker parameters, such as plasma taurine and the glutamine/glutamate ratios, showed little normalization across most patients, and the long-term clinical significance of these observations requires further investigation. There was a high degree of interindividual variability in the follow-up patients, which may reflect the heterogeneity of PACS as an emergent clinical syndrome. At present, it is unclear whether PACS is the terminal extension of the COVID-19 disease trajectory or indeed the emergence of collateral onset of additional separate disease entities. The observation of increased levels of 3-indole acetic acid implies a microbiome functionality shift in the post-acute COVID-19 patients; this may also be pertinent to understanding the tryptophan pathway perturbations in PACS patients given the general importance of the microbiome in tryptophan metabolism and serotonin production. Larger studies with greater ranges of observed severity should cast further light on the ability to determine predictors of PACS and the individual patterns of longer-term symptoms exhibited by patients. Heterogeneous metabotype patterns were observed for the PACS patient spectrum, and if reflective of the clinical picture, these could enable personalized interpretation of the persisting inflammatory/metabolic abnormalities and give insights into strategies for long-term disease mitigation in affected individuals. Worldwide, over 160 million have been infected by the SARS-CoV-2 virus so far, with 138 million so-called "recovered" patients, of whom many tens of millions are likely to have PACS with multiple-organ involvements. It is therefore important to find metabolic markers that illuminate possible public healthcare "time-bombs" for future medico-economic burdens that may be faced by many societies as a result of widespread exposure of populations to the disease. The current data and models provide the basis for a framework of assessment of the extent of multifunctional biochemical patient recovery from COVID-19. With further refinement, including addition of other metabolic system parameters, new biomarker panels can be assembled to assess patients with PACS and assist in clinical decision making in their long-term management and disease mitigation.

https://doi.org/10.1021/acs.jproteome.1c00224
J. Proteome Res. 2021, 20, 3315−3329

■ ASSOCIATED CONTENT

Supporting Information

The Supporting Information is available free of charge at https://pubs.acs.org/doi/10.1021/acs.jproteome.1c00224.

List of parameters considered from targeted MS assays (Table S1); list of parameters considered from IVDr lipoproteins (Table S2); list of parameters considered from IVDr small molecules (Table S3); list of parameters considered from DIRE-NMR experiments (Table S4); demographic information about the population of the recovery cohort (Table S5); description of the number of samples (patients) included in each method (Table S6); univariate statistics: 3-hydroxykynurenine (Figure S1), 3-hydroxykynurenine/kynurenic acid (Figure S2), aspartic acid (Figure S3), citrulline (Figure S4), Fisher's ratio (Figure S5), glutamic acid (Figure S6), glutamine/glutamic acid (Figure S7), histidine (Figure S8), indole-3-acetic acid (Figure S9), kynurenine (Figure S10), kynurenine/tryptophan (Figure S11), neopterin (Figure S12), phenylalanine (Figure S13), phenylalanine/tyrosine (Figure S14), quinolinic acid (Figure S15), quinolinic acid/kynurenic acid (Figure S16), taurine (Figure S17), and tryptophan (Figure S18); correlation using the healthy population ordered according to hierarchical clustering obtained from healthy control (Figure S19); correlation using the positive population ordered according to hierarchical clustering obtained from healthy control (Figure S20); correlation using the recovered population ordered according to hierarchical clustering obtained from healthy control (Figure S21); univariate statistics: ABA1 (Figure S22), H1FC (Figure S23), H2A1 (Figure S24), H2FC (Figure S25), H3A1 (Figure S26), H3CH (Figure S27), H3FC (Figure S28), H3PL (Figure S29), H4A1 (Figure S30), H4A2 (Figure S31), H4CH (Figure S32), H4FC (Figure S33), H4PL (Figure S34), HDA1 (Figure S35), HDA2 (Figure S36), HDCH (Figure S37), HDFC (Figure S38), HDPL (Figure S39), IDAB (Figure S40), IDPN (Figure S41), L2TG (Figure S42), L4TG (Figure S43), L5TG (Figure S44), LDHD (Figure S45), LDTG (Figure S46), TPA1 (Figure S47), TPA2 (Figure S48), TPCH (Figure S49), and V4FC (Figure S50); correlation using the healthy population ordered according to hierarchical clustering (Figure S51); correlation using the positive population ordered according to hierarchical clustering obtained from healthy control (Figure S52); correlation using the recovered population ordered according to hierarchical clustering obtained from healthy control (Figure S53); univariate statistics: glucose (Figure S54), GlycA (Figure S55), GlycB (Figure S56), SPC_{total} (Figure S57), and SPC_{total}/GlycA (Figure S58) (PDF)

■ AUTHOR INFORMATION

Corresponding Authors

Elaine Holmes − *Australian National Phenome Centre, Health Futures Institute, Murdoch University, Perth, WA 6150, Australia; Center for Computational and Systems Medicine, Health Futures Institute, Murdoch University, Perth, WA 6150, Australia; Department of Metabolism, Digestion, and Reproduction, Faculty of Medicine, Imperial College London, London SW7 2AZ, U.K.;* orcid.org/0000-0002-0556-8389; Email: elaine.holmes@murdoch.edu.au

Julien Wist − *Australian National Phenome Centre, Health Futures Institute, Murdoch University, Perth, WA 6150, Australia; Center for Computational and Systems Medicine, Health Futures Institute, Murdoch University, Perth, WA 6150, Australia; Chemistry Department, Universidad del Valle, 76001 Cali, Colombia;* orcid.org/0000-0002-3416-2572; Email: julien.wist@murdoch.edu.au, julien.wist@correounivalle.edu.co

Jeremy K. Nicholson − *Australian National Phenome Centre, Health Futures Institute, Murdoch University, Perth, WA 6150, Australia; Center for Computational and Systems Medicine, Health Futures Institute, Murdoch University, Perth, WA 6150, Australia; Institute of Global Health Innovation, Imperial College London, London SW7 2AZ, U.K.;* orcid.org/0000-0002-8123-8349; Email: Jeremy.nicholson@murdoch.edu.au, j.nicholson@imperial.ac.uk

Authors

Reika Masuda − *Australian National Phenome Centre, Health Futures Institute, Murdoch University, Perth, WA 6150, Australia*

Samantha Lodge − *Australian National Phenome Centre, Health Futures Institute, Murdoch University, Perth, WA 6150, Australia; Center for Computational and Systems Medicine, Health Futures Institute, Murdoch University, Perth, WA 6150, Australia;* orcid.org/0000-0001-9193-0462

Philipp Nitschke − *Australian National Phenome Centre, Health Futures Institute, Murdoch University, Perth, WA 6150, Australia*

Torben Kimhofer − *Australian National Phenome Centre, Health Futures Institute, Murdoch University, Perth, WA 6150, Australia; Center for Computational and Systems Medicine, Health Futures Institute, Murdoch University, Perth, WA 6150, Australia;* orcid.org/0000-0001-7158-9930

Ruey Leng Loo − *Center for Computational and Systems Medicine, Health Futures Institute, Murdoch University, Perth, WA 6150, Australia;* orcid.org/0000-0001-5307-5709

Sofina Begum − *Department of Metabolism, Digestion, and Reproduction, Faculty of Medicine, Imperial College London, London SW7 2AZ, U.K.*

Berin Boughton − *Australian National Phenome Centre, Health Futures Institute, Murdoch University, Perth, WA 6150, Australia; Center for Computational and Systems Medicine, Health Futures Institute, Murdoch University, Perth, WA 6150, Australia;* orcid.org/0000-0001-6342-9814

Rongchang Yang − *Australian National Phenome Centre, Health Futures Institute, Murdoch University, Perth, WA 6150, Australia*

Aude-Claire Morillon − *Australian National Phenome Centre, Health Futures Institute, Murdoch University, Perth, WA 6150, Australia*

Sung-Tong Chin − *Australian National Phenome Centre, Health Futures Institute, Murdoch University, Perth, WA 6150, Australia*

Drew Hall − *Australian National Phenome Centre, Health Futures Institute, Murdoch University, Perth, WA 6150, Australia*

Monique Ryan − *Australian National Phenome Centre, Health Futures Institute, Murdoch University, Perth, WA 6150, Australia*

https://doi.org/10.1021/acs.jproteome.1c00224
J. Proteome Res. 2021, 20, 3315−3329

Sze-How Bong − *Australian National Phenome Centre, Health Futures Institute, Murdoch University, Perth, WA 6150, Australia;* orcid.org/0000-0002-3313-5097
Melvin Gay − *Bruker Pty. Ltd., Preston, VIC 3072, Australia*
Dale W. Edgar − *State Adult Burn Unit, Fiona Stanley Hospital, Murdoch, WA 6150, Australia; Burn Injury Research Node, The University of Notre Dame, Fremantle, WA 6160, Australia*
John C. Lindon − *Department of Surgery and Cancer, Faculty of Medicine, Imperial College London, London SW7 2AZ, U.K.;* orcid.org/0000-0002-0916-6360
Toby Richards − *Department of Surgery, Fiona Stanley Hospital, Medical School, University of Western Australia, Perth, WA 6150, Australia*
Bu B. Yeap − *Department of Endocrinology and Diabetes, Fiona Stanley Hospital, Medical School, University of Western Australia, Perth, WA 6150, Australia*
Sven Pettersson − *Singapore National NeuroScience Centre, Singapore 308232, Singapore; Lee Kong Chian School of Medicine, Nanyang Technological University, Singapore 308232, Singapore; Department of Life Science Centre, Sunway University, Kuala Lumpur 47500, Malaysia*
Manfred Spraul − *Bruker Biospin GmbH, Ettlingen 76275, Germany*
Hartmut Schaefer − *Bruker Biospin GmbH, Ettlingen 76275, Germany*
Nathan G. Lawler − *Australian National Phenome Centre, Health Futures Institute, Murdoch University, Perth, WA 6150, Australia; Center for Computational and Systems Medicine, Health Futures Institute, Murdoch University, Perth, WA 6150, Australia;* orcid.org/0000-0001-9649-425X
Nicola Gray − *Australian National Phenome Centre, Health Futures Institute, Murdoch University, Perth, WA 6150, Australia; Center for Computational and Systems Medicine, Health Futures Institute, Murdoch University, Perth, WA 6150, Australia;* orcid.org/0000-0002-0094-5245
Luke Whiley − *Australian National Phenome Centre, Health Futures Institute, Murdoch University, Perth, WA 6150, Australia; Perron Institute for Neurological and Translational Science, Nedlands, WA 6009, Australia;* orcid.org/0000-0002-9088-4799

Complete contact information is available at: https://pubs.acs.org/10.1021/acs.jproteome.1c00224

Notes

The authors declare no competing financial interest.
The original data of the follow up cohort can be found at DOI:10.5281/zenodo.4713391.

■ ACKNOWLEDGMENTS

We thank The Spinnaker Health Research Foundation, WA, The McCusker Foundation, WA, The Western Australian State Government, and the MRFF for funding the Australian National Phenome Centre for this and related work. We thank the UK MRC for funding (S.B.), the Department of Jobs, Tourism, Science and Innovation, Government of Western Australian Premier's Fellowship for funding R.-L.L. and E.H., and the ARC Laureate Fellowship funding for E.H. We also would like to acknowledge the Western Australian Covid Research Response team (https://research-au.net/covid-research-response/), Dale Edgar, Giuliana D'Aulerio, Kelly Beer, Rolee Kumar, Doug Robb, Joseph Miocevich, Dominic Mallonic, Michael Epis, Merrilee Needham, Daniel Fatovich, Aron Chakera, Thomas Gilbert, Nathanael Foo, @STRIVE WA, Candice Peel, Sheeraz Mohd, and Ali Alishum for the coordination, sampling, and biobanking of patient samples and clinical metadata. The TOC figure was created using BioRender.com (an individual account that is suitable for publication in journal and commercial purposes).

■ REFERENCES

(1) Lopez-Leon, S.; Wegman-Ostrosky, T.; Perelman, C.; Sepulveda, R.; Rebolledo, P.; Cuapio, A.; Villapol, S. More Than 50 Long-Term Effects of COVID-19: A Systematic Review and Meta-Analysis. *Res. Square* **2021**, DOI: 10.21203/rs.3.rs-266574/v1.
(2) Carfì, A.; Bernabei, R.; Landi, F. Gemelli Against COVID-19 Post-Acute Care Study Group. Persistent Symptoms in Patients After Acute COVID-19. *JAMA* **2020**, *324*, 603−605.
(3) Goërtz, Y. M. J.; Van Herck, M.; Delbressine, J. M.; Vaes, A. W.; Meys, R.; Machado, F. V. C.; Houben-Wilke, S.; Burtin, C.; Posthuma, R.; Franssen, F. M. E.; van Loon, N.; Hajian, B.; Spies, Y.; Vijlbrief, H.; van't Hul, A. J.; Janssen, D. J. A.; Spruit, M. A. Persistent Symptoms 3 Months after a SARS-CoV-2 Infection: The Post-COVID-19 Syndrome? *ERJ Open Res.* **2020**, *6*, 00542−02020.
(4) Raman, B.; Cassar, M. P.; Tunnicliffe, E. M.; Filippini, N.; Griffanti, L.; Alfaro-Almagro, F.; Okell, T.; Sheerin, F.; Xie, C.; Mahmod, M.; Mózes, F. E.; Lewandowski, A. J.; Ohuma, E. O.; Holdsworth, D.; Lamlum, H.; Woodman, M. J.; Krasopoulos, C.; Mills, R.; McConnell, F. A. K.; Wang, C.; Arthofer, C.; Lange, F. J.; Andersson, J.; Jenkinson, M.; Antoniades, C.; Channon, K. M.; Shanmuganathan, M.; Ferreira, V. M.; Piechnik, S. K.; Klenerman, P.; Brightling, C.; Talbot, N. P.; Petousi, N.; Rahman, N. M.; Ho, L.-P.; Saunders, K.; Geddes, J. R.; Harrison, P. J.; Pattinson, K.; Rowland, M. J.; Angus, B. J.; Gleeson, F.; Pavlides, M.; Koychev, I.; Miller, K. L.; Mackay, C.; Jezzard, P.; Smith, S. M.; Neubauer, S. Medium-Term Effects of SARS-CoV-2 Infection on Multiple Vital Organs, Exercise Capacity, Cognition, Quality of Life and Mental Health, Post-Hospital Discharge. *EClinicalMedicine* **2021**, *31*, No. 100683.
(5) Mandal, S.; Barnett, J.; Brill, S. E.; Brown, J. S.; Denneny, E. K.; Hare, S. S.; Heightman, M.; Hillman, T. E.; Jacob, J.; Jarvis, H. C.; Lipman, M. C. I.; Naidu, S. B.; Nair, A.; Porter, J. C.; Tomlinson, G. S.; Hurst, J. R.; ARC Study Group. "Long-COVID": A Cross-Sectional Study of Persisting Symptoms, Biomarker and Imaging Abnormalities Following Hospitalisation for COVID-19. *Thorax* **2021**, *76*, 396−398.
(6) Woo, M. S.; Malsy, J.; Pöttgen, J.; Seddiq Zai, S.; Ufer, F.; Hadjilaou, A.; Schmiedel, S.; Addo, M. M.; Gerloff, C.; Heesen, C.; Schulze Zur Wiesch, J.; Friese, M. A. Frequent Neurocognitive Deficits after Recovery from Mild COVID-19. *Brain Commun.* **2020**, *2*, No. fcaa205.
(7) Niklassen, A. S.; Draf, J.; Huart, C.; Hintschich, C.; Bocksberger, S.; Trecca, E. M. C.; Klimek, L.; Le Bon, S. D.; Altundag, A.; Hummel, T. COVID-19: Recovery from Chemosensory Dysfunction. A Multicentre Study on Smell and Taste. *Laryngoscope* **2021**, *131*, 1095−1100.
(8) Puntmann, V. O.; Carerj, M. L.; Wieters, I.; Fahim, M.; Arendt, C.; Hoffmann, J.; Shchendrygina, A.; Escher, F.; Vasa-Nicotera, M.; Zeiher, A. M.; Vehreschild, M.; Nagel, E. Outcomes of Cardiovascular Magnetic Resonance Imaging in Patients Recently Recovered From Coronavirus Disease 2019 (COVID-19). *JAMA Cardiol.* **2020**, *5*, 1265−1273.
(9) An, Y.-W.; Song, S.; Li, W.-X.; Chen, Y.-X.; Hu, X.-P.; Zhao, J.; Li, Z.-W.; Jiang, G.-Y.; Wang, C.; Wang, J.-C.; Yuan, B.; Liu, H.-Q. Liver Function Recovery of COVID-19 Patients after Discharge, a Follow-up Study. *Int. J. Med. Sci.* **2021**, *18*, 176−186.
(10) McMahon, D. E.; Gallman, A. E.; Hruza, G. J.; Rosenbach, M.; Lipoff, J. B.; Desai, S. R.; French, L. E.; Lim, H.; Cyster, J. G.; Fox, L. P.; Fassett, M. S.; Freeman, E. E. Long COVID in the Skin: A Registry Analysis of COVID-19 Dermatological Duration. *Lancet Infect. Dis.* **2021**, *21*, 313−314.
(11) Cañas, C. A. The Triggering of Post-COVID-19 Autoimmunity Phenomena Could Be Associated with Both Transient Immunosup-

pression and an Inappropriate Form of Immune Reconstitution in Susceptible Individuals. *Med. Hypotheses* **2020**, *145*, No. 110345.
(12) Rubino, F.; Amiel, S. A.; Zimmet, P.; Alberti, G.; Bornstein, S.; Eckel, R. H.; Mingrone, G.; Boehm, B.; Cooper, M. E.; Chai, Z.; Del Prato, S.; Ji, L.; Hopkins, D.; Herman, W. H.; Khunti, K.; Mbanya, J. C.; Renard, E. New-Onset Diabetes in Covid-19. *N. Engl. J. Med.* **2020**, *383*, 789−790.
(13) Thepmankorn, P.; Bach, J.; Lasfar, A.; Zhao, X.; Souayah, S.; Chong, Z. Z.; Souayah, N. Cytokine Storm Induced by SARS-CoV-2 Infection: The Spectrum of Its Neurological Manifestations. *Cytokine* **2021**, *138*, No. 155404.
(14) Coperchini, F.; Chiovato, L.; Croce, L.; Magri, F.; Rotondi, M. The Cytokine Storm in COVID-19: An Overview of the Involvement of the Chemokine/chemokine-Receptor System. *Cytokine Growth Factor Rev.* **2020**, *53*, 25−32.
(15) Hui, D. S. C.; Wong, K. T.; Antonio, G. E.; Tong, M.; Chan, D. P.; Sung, J. J. Y. Long-Term Sequelae of SARS: Physical, Neuropsychiatric, and Quality-of-Life Assessment. *Hong Kong Med. J.* **2009**, *15*, 21−23.
(16) O'Sullivan, O. Long-Term Sequelae Following Previous Coronavirus Epidemics. *Clin. Med.* **2021**, *21*, e68−e70.
(17) Huang, C.; Huang, L.; Wang, Y.; Li, X.; Ren, L.; Gu, X.; Kang, L.; Guo, L.; Liu, M.; Zhou, X.; Luo, J.; Huang, Z.; Tu, S.; Zhao, Y.; Chen, L.; Xu, D.; Li, Y.; Li, C.; Peng, L.; Li, Y.; Xie, W.; Cui, D.; Shang, L.; Fan, G.; Xu, J.; Wang, G.; Wang, Y.; Zhong, J.; Wang, C.; Wang, J.; Zhang, D.; Cao, B. 6-Month Consequences of COVID-19 in Patients Discharged from Hospital: A Cohort Study. *Lancet* **2021**, *397*, 220−232.
(18) Bindu, S.; Mazumder, S.; Bandyopadhyay, U. Non-Steroidal Anti-Inflammatory Drugs (NSAIDs) and Organ Damage: A Current Perspective. *Biochem. Pharmacol.* **2020**, *180*, No. 114147.
(19) Guedj, E.; Campion, J. Y.; Dudouet, P.; Kaphan, E.; Bregeon, F.; Tissot-Dupont, H.; Guis, S.; Barthelemy, F.; Habert, P.; Ceccaldi, M.; Million, M.; Raoult, D.; Cammilleri, S.; Eldin, C. 18F-FDG Brain PET Hypometabolism in Patients with Long COVID. *Eur. J. Nucl. Med. Mol. Imaging* **2021**, 1−11.
(20) Townsend, L.; Fogarty, H.; Dyer, A.; Martin-Loeches, I.; Bannan, C.; Nadarajan, P.; Bergin, C.; O'Farrelly, C.; Conlon, N.; Bourke, N. M.; Ward, S. E.; Byrne, M.; Ryan, K.; O'Connell, N.; O'Sullivan, J. M.; Ni Cheallaigh, C.; O'Donnell, J. S. Prolonged Elevation of D-Dimer Levels in Convalescent COVID-19 Patients Is Independent of the Acute Phase Response. *J. Thromb. Haemost.* **2021**, *19*, 1064−1070.
(21) The Lancet. Facing up to Long COVID. *Lancet* **2020**, *396*, 1861.
(22) Nalbandian, A.; Sehgal, K.; Gupta, A.; Madhavan, M. V.; McGroder, C.; Stevens, J. S.; Cook, J. R.; Nordvig, A. S.; Shalev, D.; Sehrawat, S.; Ahluwalia, N.; Bikdeli, B.; Dietz, D.; Der-Nigoghossian, C.; Liyanage-Don, N.; Rosner, G. F.; Bernstein, E. J.; Mohan, S.; Beckley, A. A.; Seres, D. S.; Choueiri, T. K.; Uriel, N.; Ausiello, J. C.; Accili, D.; Freedberg, D. E.; Baldwin, M.; Schwartz, A.; Brodie, D.; Garcia, C. K.; Elkind, M. S. V.; Connors, J. M.; Bilezikian, J. P.; Landry, D. W.; Wan, E. Y. Post-acute COVID-19 Syndrome. *Nat. Med.* **2021**, *27*, 601−615.
(23) Kimhofer, T.; Lodge, S.; Whiley, L.; Gray, N.; Loo, R. L.; Lawler, N. G.; Nitschke, P.; Bong, S. H.; Morrison, D. L.; Begum, S.; Richards, T.; Yeap, B. B.; Smith, C.; Smith, K. C. G.; Holmes, E.; Nicholson, J. K. Integrative Modelling of Quantitative Plasma Lipoprotein, Metabolic and Amino Acid Data Reveals a Multi-Organ Pathological Signature of SARS-CoV-2 Infection. *J. Proteome Res.* **2020**, *19*, 4442−4454.
(24) Lodge, S.; Nitschke, P.; Kimhofer, T.; Coudert, J. D.; Begum, S.; Bong, S.-H.; Richards, T.; Edgar, D.; Raby, E.; Spraul, M.; Schaefer, H.; Lindon, J. C.; Loo, R. L.; Holmes, E.; Nicholson, J. K. NMR Spectroscopic Windows on the Systemic Effects of SARS-CoV-2 Infection on Plasma Lipoproteins and Metabolites in Relation to Circulating Cytokines. *J. Proteome Res.* **2021**, *20*, 1382−1396.
(25) Shen, B.; Yi, X.; Sun, Y.; Bi, X.; Du, J.; Zhang, C.; Quan, S.; Zhang, F.; Sun, R.; Qian, L.; Ge, W.; Liu, W.; Liang, S.; Chen, H.; Zhang, Y.; Li, J.; Xu, J.; He, Z.; Chen, B.; Wang, J.; Yan, H.; Zheng, Y.; Wang, D.; Zhu, J.; Kong, Z.; Kang, Z.; Liang, X.; Ding, X.; Ruan, G.; Xiang, N.; Cai, X.; Gao, H.; Li, L.; Li, S.; Xiao, Q.; Lu, T.; Zhu, Y.; Liu, H.; Chen, H.; Guo, T. Proteomic and Metabolomic Characterization of COVID-19 Patient Sera. *Cell* **2020**, *182*, 59.e15−72.e15.
(26) Lawler, N. G.; Gray, N.; Kimhofer, T.; Boughton, B.; Gay, M.; Yang, R.; Morillon, A.-C.; Chin, S.-T.; Ryan, M.; Begum, S.; Bong, S. H.; Coudert, J. D.; Edgar, D.; Raby, E.; Pettersson, S.; Richards, T.; Holmes, E.; Whiley, L.; Nicholson, J. K. Systemic Perturbations in Amine and Kynurenine Metabolism Associated with Acute SARS-CoV-2 Infection and Inflammatory Cytokine Responses. *J. Proteome Res.* **2021**, *20* (5), 2796−2811, DOI: 10.1021/acs.jproteome.1c00052.
(27) Bruzzone, C.; Bizkarguenaga, M.; Gil-Redondo, R.; Diercks, T.; Arana, E.; García de Vicuña, A.; Seco, M.; Bosch, A.; Palazón, A.; San Juan, I.; Laín, A.; Gil-Martínez, J.; Bernardo-Seisdedos, G.; Fernández-Ramos, D.; Lopitz-Otsoa, F.; Embade, N.; Lu, S.; Mato, J. M.; Millet, O. SARS-CoV-2 Infection Dysregulates the Metabolomic and Lipidomic Profiles of Serum. *iScience* **2020**, *23*, No. 101645.
(28) Meoni, G.; Ghini, V.; Maggi, L.; Vignoli, A.; Mazzoni, A.; Salvati, L.; Capone, M.; Vanni, A.; Tenori, L.; Fontanari, P.; Lavorini, F.; Peris, A.; Bartoloni, A.; Liotta, F.; Cosmi, L.; Luchinat, C.; Annunziato, F.; Turano, P. Metabolomic/lipidomic Profiling of COVID-19 and Individual Response to Tocilizumab. *PLoS Pathog.* **2021**, *17*, No. e1009243.
(29) Bellan, M.; Soddu, D.; Balbo, P. E.; Baricich, A.; Zeppegno, P.; Avanzi, G. C.; Baldon, G.; Bartolomei, G.; Battaglia, M.; Battistini, S.; Binda, V.; Borg, M.; Cantaluppi, V.; Castello, L. M.; Clivati, E.; Cisari, C.; Costanzo, M.; Croce, A.; Cuneo, D.; De Benedittis, C.; De Vecchi, S.; Feggi, A.; Gai, M.; Gambaro, E.; Gattoni, E.; Gramaglia, C.; Grisafi, L.; Guerriero, C.; Hayden, E.; Jona, A.; Invernizzi, M.; Lorenzini, L.; Loreti, L.; Martelli, M.; Marzullo, P.; Matino, E.; Panero, A.; Parachini, E.; Patrucco, F.; Patti, G.; Pirovano, A.; Prosperini, P.; Quaglino, R.; Rigamonti, C.; Sainaghi, P. P.; Vecchi, C.; Zecca, E.; Pirisi, M. Respiratory and Psychophysical Sequelae Among Patients With COVID-19 Four Months After Hospital Discharge. *JAMA Network Open* **2021**, *4*, No. e2036142.
(30) Liao, B.; Liu, Z.; Tang, L.; Li, L.; Gan, Q.; Shi, H.; Jiao, Q.; Guan, Y.; Xie, M.; He, X.; Zhao, H.; Chen, W.; Liu, Y.; Li, L.; Wang, Y.; Cao, Y.; Shi, Y.; Li, Y.; Lei, C. Longitudinal Clinical and Radiographic Evaluation Reveals Interleukin-6 as an Indicator of Persistent Pulmonary Injury in COVID-19. *Int. J. Med. Sci.* **2021**, *18*, 29−41.
(31) Stavem, K.; Ghanima, W.; Olsen, M. K.; Gilboe, H. M.; Einvik, G. Persistent Symptoms 1.5-6 Months after COVID-19 in Non-Hospitalised Subjects: A Population-Based Cohort Study. *Thorax* **2021**, *76*, 405−407.
(32) Chan, A. T.; Drew, D. A.; Nguyen, L. H.; Joshi, A. D.; Ma, W.; Guo, C.-G.; Lo, C.-H.; Mehta, R. S.; Kwon, S.; Sikavi, D. R.; Magicheva-Gupta, M. V.; Fatehi, Z. S.; Flynn, J. J.; Leonardo, B. M.; Albert, C. M.; Andreotti, G.; Beane-Freeman, L. E.; Balasubramanian, B. A.; Brownstein, J. S.; Bruinsma, F.; Cowan, A. N.; Deka, A.; Ernst, M. E.; Figueiredo, J. C.; Franks, P. W.; Gardner, C. D.; Ghobrial, I. M.; Haiman, C. A.; Hall, J. E.; Deming-Halverson, S. L.; Kirpach, B.; Lacey, J. V., Jr.; Marchand, L. L.; Marinac, C. R.; Martinez, M. E.; Milne, R. L.; Murray, A. M.; Nash, D.; Palmer, J. R.; Patel, A. V.; Rosenberg, L.; Sandler, D. P.; Sharma, S. V.; Schurman, S. H.; Wilkens, L. R.; Chavarro, J. E.; Eliassen, A. H.; Hart, J. E.; Kang, J. H.; Koenen, K. C.; Kubzansky, L. D.; Mucci, L. A.; Ourselin, S.; Rich-Edwards, J. W.; Song, M.; Stampfer, M. J.; Steves, C. J.; Willett, W. C.; Wolf, J.; Spector, T. COPE Consortium. The COronavirus Pandemic Epidemiology (COPE) Consortium: A Call to Action. *Cancer Epidemiol. Biomarkers Prev.* **2020**, *29*, 1283−1289.
(33) Małek, A.; Marczak, M.; Miłosz-Wieczorek, B.; Konopka, M.; Braksator, W.; Drygas, W.; Krzywański, J. Cardiac Involvement in Consecutive Elite Athletes Recovered from Covid-19: A Magnetic Resonance Study. *J. Magn. Reson. Imaging* **2021**, 1−7.
(34) Harris, A.; Al Mushref, M. Graves' Thyrotoxicosis Following SARS-CoV-2 Infection. *AACE Clin. Case Rep.* **2021**, *7*, 14−16.
(35) Mehmood, M. A.; Bapna, M.; Arshad, M. A Case of Post-COVID-19 Subacute Thyroiditis. *Cureus* **2020**, *12*, No. e12301.
(36) Mattar, S. A. M.; Koh, S. J. Q.; Rama Chandran, S.; Cherng, B. P. Z. Subacute Thyroiditis Associated with COVID-19. *BMJ Case Rep.* **2020**, *13*, No. e237336.

(37) Alnafiey, M. O.; Alangari, A. M.; Alarifi, A. M.; Abushara, A. Persistent Hypokalemia Post SARS-coV-2 Infection, Is It a Life-Long Complication? Case Report. *Ann. Med. Surg.* **2021**, *62*, 358−361.
(38) Printza, A.; Katotomichelakis, M.; Metallidis, S.; Panagopoulos, P.; Sarafidou, A.; Petrakis, V.; Constantinidis, J. The Clinical Course of Smell and Taste Loss in COVID-19 Hospitalized Patients. *Hippokratia* **2020**, *24*, 66−71.
(39) Simani, L.; Ramezani, M.; Darazam, I. A.; Sagharichi, M.; Aalipour, M. A.; Ghorbani, F.; Pakdaman, H. Prevalence and Correlates of Chronic Fatigue Syndrome and Post-Traumatic Stress Disorder after the Outbreak of the COVID-19. *J. NeuroVirol.* **2021**, *27*, 154−159.
(40) Akter, F.; Mannan, A.; Mehedi, H. M. H.; Rob, M. A.; Ahmed, S.; Salauddin, A.; Hossain, M. S.; Hasan, M. M. Clinical Characteristics and Short Term Outcomes after Recovery from COVID-19 in Patients with and without Diabetes in Bangladesh. *Diabetes Metab. Syndr.: Clin. Res. Rev.* **2020**, *14*, 2031−2038.
(41) Sathish, T.; Kapoor, N.; Cao, Y.; Tapp, R. J.; Zimmet, P. Proportion of Newly Diagnosed Diabetes in COVID-19 Patients: A Systematic Review and Meta-Analysis. *Diabetes, Obes. Metab.* **2021**, *23*, 870−874.
(42) Clouden, T. A. Persistent Hallucinations in a 46-Year-Old Woman After COVID-19 Infection: A Case Report. *Cureus* **2020**, *12*, No. e11993.
(43) Dahl, E. H.; Mosevoll, K. A.; Cramariuc, D.; Vedeler, C. A.; Blomberg, B. COVID-19 Myocarditis and Postinfection Bell's Palsy. *BMJ Case Rep.* **2021**, *14*, No. e240095.
(44) Jali, I. Reactive Arthritis After COVID-19 Infection. *Cureus* **2020**, *12*, No. e11761.
(45) McDonnell, E. P.; Altomare, N. J.; Parekh, Y. H.; Gowda, R. C.; Parikh, P. D.; Lazar, M. H.; Blaser, M. J. COVID-19 as a Trigger of Recurrent Guillain-Barré Syndrome. *Pathogens* **2020**, *9*, No. 965.
(46) Raahimi, M. M.; Kane, A.; Moore, C. E.; Alareed, A. W. Late Onset of Guillain-Barré Syndrome Following SARS-CoV-2 Infection: Part of "Long COVID-19 Syndrome"? *BMJ Case Rep.* **2021**, *14*, No. e240178.
(47) Beckwith-Hall, B. M.; Nicholson, J. K.; Nicholls, A. W.; Foxall, P. J.; Lindon, J. C.; Connor, S. C.; Abdi, M.; Connelly, J.; Holmes, E. Nuclear Magnetic Resonance Spectroscopic and Principal Components Analysis Investigations into Biochemical Effects of Three Model Hepatotoxins. *Chem. Res. Toxicol.* **1998**, *11*, 260−272.
(48) Keun, H. C.; Ebbels, T. M.; Bollard, M. E.; Beckonert, O.; Antti, H.; Holmes, E.; Lindon, J. C.; Nicholson, J. K. Geometric Trajectory Analysis of Metabolic Responses to Toxicity Can Define Treatment Specific Profiles. *Chem. Res. Toxicol.* **2004**, *17*, 579−587.
(49) Holmes, E.; Bonner, F. W.; Sweatman, B. C.; Lindon, J. C.; Beddell, C. R.; Rahr, E.; Nicholson, J. K. Nuclear Magnetic Resonance Spectroscopy and Pattern Recognition Analysis of the Biochemical Processes Associated with the Progression of and Recovery from Nephrotoxic Lesions in the Rat Induced by mercury(II) Chloride and 2-Bromoethanamine. *Mol. Pharmacol.* **1992**, *42*, 922−930.
(50) Li, A.; Zhang, W.; Zhang, L.; Liu, Y.; Li, K.; Du, G.; Qin, X. Elucidating the Time-Dependent Changes in the Urinary Metabolome under Doxorubicin-Induced Nephrotoxicity. *Toxicol. Lett.* **2020**, *319*, 204−212.
(51) Foxall, P. J.; Bending, M. R.; Gartland, K. P.; Nicholson, J. K. Acute Renal Failure Following Accidental Cutaneous Absorption of Phenol: Application of NMR Urinalysis to Monitor the Disease Process. *Hum. Toxicol.* **1989**, *8*, 491−496.
(52) Foxall, P. J.; Mellotte, G. J.; Bending, M. R.; Lindon, J. C.; Nicholson, J. K. NMR Spectroscopy as a Novel Approach to the Monitoring of Renal Transplant Function. *Kidney Int.* **1993**, *43*, 234−245.
(53) Nicholson, J. K.; Connelly, J.; Lindon, J. C.; Holmes, E. Metabonomics: A Platform for Studying Drug Toxicity and Gene Function. *Nat. Rev. Drug Discovery* **2002**, *1*, 153−161.
(54) Lodge, S.; Nitschke, P.; Kimhofer, T.; Wist, J.; Bong, S.-H.; Loo, R. L.; Masuda, R.; Begum, S.; Richards, T.; Lindon, J. C.; Bermel, W.; Reinsperger, T.; Schaefer, H.; Spraul, M.; Holmes, E.; Nicholson, J. K. Diffusion and Relaxation Edited Proton NMR Spectroscopy of Plasma Reveals a High-Fidelity Supramolecular Biomarker Signature of SARS-CoV-2 Infection. *Anal. Chem.* **2021**, *93*, 3976−3986.
(55) Dona, A. C.; Jimenez, B.; Schafer, H.; Humpfer, E.; Spraul, M.; Lewis, M. R.; Pearce, J. T.; Holmes, E.; Lindon, J. C.; Nicholson, J. K. Precision High-Throughput Proton NMR Spectroscopy of Human Urine, Serum, and Plasma for Large-Scale Metabolic Phenotyping. *Anal. Chem.* **2014**, *86*, 9887−9894.
(56) Loo, R. L.; Lodge, S.; Kimhofer, T.; Bong, S. H.; Begum, S.; Whiley, L.; Gray, N.; Lindon, J. C.; Nitschke, P.; Lawler, N. G.; Schafer, H.; Spraul, M.; Richards, T.; Nicholson, J. K.; Holmes, E. Quantitative In-Vitro Diagnostic NMR Spectroscopy for Lipoprotein and Metabolite Measurements in Plasma and Serum: Recommendations for Analytical Artefact Minimization with Special Reference to COVID-19/SARS-CoV-2 Samples. *J. Proteome Res.* **2020**, *19*, 4428−4441.
(57) Jiménez, B.; Holmes, E.; Heude, C.; Tolson, R. F.; Harvey, N.; Lodge, S. L.; Chetwynd, A. J.; Cannet, C.; Fang, F.; Pearce, J. T. M.; Lewis, M. R.; Viant, M. R.; Lindon, J. C.; Spraul, M.; Schafer, H.; Nicholson, J. K. Quantitative Lipoprotein Subclass and Low Molecular Weight Metabolite Analysis in Human Serum and Plasma by (1)H NMR Spectroscopy in a Multilaboratory Trial. *Anal. Chem.* **2018**, *90*, 11962−11971.
(58) Gray, N.; Plumb, R. S.; Wilson, I. D.; Nicholson, J. K. A Validated UPLC-MS/MS Assay for the Quantification of Amino Acids and Biogenic Amines in Rat Urine. *J. Chromatogr. B: Anal. Technol. Biomed. Life Sci.* **2019**, *1106−1107*, 50−57.
(59) Gray, N.; Lawler, N. G.; Yang, R.; Morillon, A.-C.; Gay, M. C. L.; Bong, S.-H.; Holmes, E.; Nicholson, J. K.; Whiley, L. A Simultaneous Exploratory and Quantitative Amino Acid and Biogenic Amine Metabolic Profiling Platform for Rapid Disease Phenotyping via UPLC-QToF-MS. *Talanta* **2021**, *223*, No. 121872.
(60) Whiley, L.; Nye, L. C.; Grant, I.; Andreas, N.; Chappell, K. E.; Sarafian, M. H.; Misra, R.; Plumb, R. S.; Lewis, M. R.; Nicholson, J. K.; Holmes, E.; Swann, J. R.; Wilson, I. D. Ultrahigh-Performance Liquid Chromatography Tandem Mass Spectrometry with Electrospray Ionization Quantification of Tryptophan Metabolites and Markers of Gut Health in Serum and Plasma-Application to Clinical and Epidemiology Cohorts. *Anal. Chem.* **2019**, *91*, 5207−5216.
(61) Bylesjö, M.; Rantalainen, M.; Cloarec, O.; Nicholson, J. K.; Holmes, E.; Trygg, J. OPLS Discriminant Analysis: Combining the Strengths of PLS-DA and SIMCA Classification. *J. Chemom.* **2006**, *20*, 341−351.
(62) Bellmann-Weiler, R.; Lanser, L.; Burkert, F.; Seiwald, S.; Fritsche, G.; Wildner, S.; Schroll, A.; Koppelstätter, S.; Kurz, K.; Griesmacher, A.; Weiss, G. Neopterin Predicts Disease Severity in Hospitalized Patients With COVID-19. *Open Forum Infect. Dis.* **2021**, *8*, No. ofaa521.
(63) Ozger, H. S.; Dizbay, M.; Corbacioglu, S. K.; Aysert, P.; Demirbas, Z.; Tunccan, O. G.; Hizel, K.; Bozdayi, G.; Caglar, K. The Prognostic Role of Neopterin in COVID-19 Patients. *J. Med. Virol.* **2021**, *93*, 1520−1525.
(64) Zheng, B.; Cao, K.-Y.; Chan, C. P. Y.; Choi, J. W. Y.; Leung, W.; Leung, M.; Duan, Z.-H.; Gao, Y.; Wang, M.; Di, B.; Hollidt, J. M.; Bergmann, A.; Lehmann, M.; Renneberg, I.; Tam, J. S. L.; Chan, P. K. S.; Cautherley, G. W. H.; Fuchs, D.; Renneberg, R. Serum Neopterin for Early Assessment of Severity of Severe Acute Respiratory Syndrome. *Clin. Immunol.* **2005**, *116*, 18−26.
(65) Korecka, A.; Dona, A.; Lahiri, S.; Tett, A. J.; Al-Asmakh, M.; Braniste, V.; D'Arienzo, R.; Abbaspour, A.; Reichardt, N.; Fujii-Kuriyama, Y.; Rafter, J.; Narbad, A.; Holmes, E.; Nicholson, J.; Arulampalam, V.; Pettersson, S. Bidirectional Communication between the Aryl Hydrocarbon Receptor (AhR) and the Microbiome Tunes Host Metabolism. *NPJ Biofilms Microbiomes* **2016**, *2*, No. 16014.
(66) Hendrikx, T.; Schnabl, B. Indoles: Metabolites Produced by Intestinal Bacteria Capable of Controlling Liver Disease Manifestation. *J. Intern. Med.* **2019**, *286*, 32−40.
(67) Fahlberg, M. D.; Blair, R. V.; Doyle-Meyers, L. A.; Midkiff, C. C.; Zenere, G.; Russell-Lodrigue, K. E.; Monjure, C. J.; Haupt, E. H.; Penney, T. P.; Lehmicke, G.; Threeton, B. M.; Golden, N.; Datta, P. K.; Roy, C. J.; Bohm, R. P.; Maness, N. J.; Fischer, T.; Rappaport, J.; Vaccari, M. Cellular Events of Acute, Resolving or Progressive COVID-

https://doi.org/10.1021/acs.jproteome.1c00224
J. Proteome Res. 2021, 20, 3315−3329

19 in SARS-CoV-2 Infected Non-Human Primates. *Nat. Commun.* **2020**, *11*, No. 6078.
(68) Lionetto, L.; Ulivieri, M.; Capi, M.; De Bernardini, D.; Fazio, F.; Petrucca, A.; Pomes, L. M.; De Luca, O.; Gentile, G.; Casolla, B.; Curto, M.; Salerno, G.; Schillizzi, S.; Torre, M. S.; Santino, I.; Rocco, M.; Marchetti, P.; Aceti, A.; Ricci, A.; Bonfini, R.; Nicoletti, F.; Simmaco, M.; Borro, M. Increased Kynurenine-to-Tryptophan Ratio in the Serum of Patients Infected with SARS-CoV2: An Observational Cohort Study. *Biochim. Biophys. Acta, Mol. Basis Dis.* **2021**, *1867*, No. 166042.
(69) Widner, B.; Leblhuber, F.; Fuchs, D. Increased Neopterin Production and Tryptophan Degradation in Advanced Parkinson's Disease. *J. Neural Transm.* **2002**, *109*, 181−189.
(70) Yu, E.; Papandreou, C.; Ruiz-Canela, M.; Guasch-Ferre, M.; Clish, C. B.; Dennis, C.; Liang, L.; Corella, D.; Fitó, M.; Razquin, C.; Lapetra, J.; Estruch, R.; Ros, E.; Cofán, M.; Arós, F.; Toledo, E.; Serra-Majem, L.; Sorlí, J. V.; Hu, F. B.; Martinez-Gonzalez, M. A.; Salas-Salvado, J. Association of Tryptophan Metabolites with Incident Type 2 Diabetes in the PREDIMED Trial: A Case-Cohort Study. *Clin. Chem.* **2018**, *64*, 1211−1220.
(71) Dagenais-Lussier, X.; Loucif, H.; Beji, C.; Telittchenko, R.; Routy, J.-P.; van Grevenynghe, J. Latest Developments in Tryptophan Metabolism: Understanding Its Role in B Cell Immunity. *Cytokine Growth Factor Rev.* **2021**, 1359−6101.
(72) Åkesson, K.; Pettersson, S.; Ståhl, S.; Surowiec, I.; Hedenström, M.; Eketjäll, S.; Trygg, J.; Jakobsson, P.-J.; Gunnarsson, I.; Svenungsson, E.; Idborg, H. Kynurenine Pathway Is Altered in Patients with SLE and Associated with Severe Fatigue. *Lupus Sci. Med.* **2018**, *5*, No. e000254.
(73) Dhillon, A. K.; Rupp, C.; Bergquist, A.; Voitl, R.; Folseraas, T.; Trøseid, M.; Midttun, Ø.; Ueland, P. M.; Karlsen, T. H.; Vesterhus, M.; Kummen, M.; Hov, J. R. Associations of Neopterin and Kynurenine-Tryptophan Ratio with Survival in Primary Sclerosing Cholangitis. *Scand. J. Gastroenterol.* **2021**, 443−452.
(74) Lu, C.; Wang, Y.; Sheng, Z.; Liu, G.; Fu, Z.; Zhao, J.; Zhao, J.; Yan, X.; Zhu, B.; Peng, S. NMR-Based Metabonomic Analysis of the Hepatotoxicity Induced by Combined Exposure to PCBs and TCDD in Rats. *Toxicol. Appl. Pharmacol.* **2010**, *248*, 178−184.
(75) Schuller-Levis, G. B.; Park, E. Taurine: New Implications for an Old Amino Acid. *FEMS Microbiol. Lett.* **2003**, *226*, 195−202.
(76) Spriet, L. L.; Whitfield, J. Taurine and Skeletal Muscle Function. *Curr. Opin. Clin. Nutr. Metab. Care* **2015**, *18*, 96−101.
(77) Nanobashvili, J.; Neumayer, C.; Fügl, A.; Punz, A.; Blumer, R.; Prager, M.; Mittlböck, M.; Gruber, H.; Polterauer, P.; Roth, E.; Malinski, T.; Huk, I. Ischemia/reperfusion Injury of Skeletal Muscle: Plasma Taurine as a Measure of Tissue Damage. *Surgery* **2003**, *133*, 91−100.
(78) Gonzalez, A.; Orozco-Aguilar, J.; Achiardi, O.; Simon, F.; Cabello-Verrugio, C. SARS-CoV-2/Renin-Angiotensin System: Deciphering the Clues for a Couple with Potentially Harmful Effects on Skeletal Muscle. *Int. J. Mol. Sci.* **2020**, *21*, No. 7904.
(79) Doğan, H. O.; Şenol, O.; Bolat, S.; Yıldız, Ş. N.; Büyüktuna, S. A.; Sarıismailoğlu, R.; Doğan, K.; Hasbek, M.; Hekim, S. N. Understanding the Pathophysiological Changes via Untargeted Metabolomics in COVID-19 Patients. *J. Med. Virol.* **2021**, *93*, 2340−2349.
(80) Tran-Dinh, S.; Hoerter, J. A.; Mateo, P.; Bouet, F.; Herve, M. A Simple Mathematical Model and Practical Approach for Evaluating Citric Acid Cycle Fluxes in Perfused Rat Hearts by 13C-NMR and 1H-NMR Spectroscopy. *Eur. J. Biochem.* **1997**, *245*, 497−504.
(81) Gavriatopoulou, M.; Korompoki, E.; Fotiou, D.; Ntanasis-Stathopoulos, I.; Psaltopoulou, T.; Kastritis, E.; Terpos, E.; Dimopoulos, M. A. Organ-Specific Manifestations of COVID-19 Infection. *Clin. Exp. Med.* **2020**, *20*, 493−506.
(82) Lau, A.; Tymianski, M. Glutamate Receptors, Neurotoxicity and Neurodegeneration. *Pflugers Arch.* **2010**, *460*, 525−542.
(83) Stone, T. W. Endogenous Neurotoxins from Tryptophan. *Toxicon* **2001**, *39*, 61−73.
(84) Heilman, P. L.; Wang, E. W.; Lewis, M. M.; Krzyzanowski, S.; Capan, C. D.; Burmeister, A. R.; Du, G.; Escobar Galvis, M. L.; Brundin, P.; Huang, X.; Brundin, L. Tryptophan Metabolites Are Associated With Symptoms and Nigral Pathology in Parkinson's Disease. *Mov. Disord.* **2020**, *35*, 2028−2037.
(85) Mahmoud, S.; Gharagozloo, M.; Simard, C.; Gris, D. Astrocytes Maintain Glutamate Homeostasis in the CNS by Controlling the Balance between Glutamate Uptake and Release. *Cells* **2019**, *8*, No. 184.
(86) Blaauw, R.; Nel, D. G.; Schleicher, G. K. Plasma Glutamine Levels in Relation to Intensive Care Unit Patient Outcome. *Nutrients* **2020**, *12*, 402.
(87) Hanif, M.; Haider, M. A.; Xi, Q.; Ali, M. J.; Ahmed, M. U. A Review of the Risk Factors Associated With Poor Outcomes in Patients With Coronavirus Disease 2019. *Cureus* **2020**, *12*, No. e10350.
(88) Lazarus, G.; Audrey, J.; Wangsaputra, V. K.; Tamara, A.; Tahapary, D. L. High Admission Blood Glucose Independently Predicts Poor Prognosis in COVID-19 Patients: A Systematic Review and Dose-Response Meta-Analysis. *Diabetes Res. Clin. Pract.* **2021**, *171*, No. 108561.
(89) Begue, F.; Tanaka, S.; Mouktadi, Z.; Rondeau, P.; Veeren, B.; Diotel, N.; Tran-Dinh, A.; Robert, T.; Vélia, E.; Mavingui, P.; Lagrange-Xélot, M.; Montravers, P.; Couret, D.; Meilhac, O. Altered High-Density Lipoprotein Composition and Functions during Severe COVID-19. *Sci. Rep.* **2021**, *11*, No. 2291.
(90) Hilser, J. R.; Han, Y.; Biswas, S.; Gukasyan, J.; Cai, Z.; Zhu, R.; Tang, W. H. W.; Deb, A.; Lusis, A. J.; Hartiala, J. A.; Allayee, H. Association of Serum HDL Cholesterol and Apolipoprotein A1 Levels with Risk of Severe SARS-CoV-2 Infection. *J. Lipid Res.* **2021**, *62*, No. 100061.
(91) Kaneva, A. M.; Potolitsyna, N. N.; Bojko, E. R.; Odland, J. Ø. The Apolipoprotein B/apolipoprotein A-I Ratio as a Potential Marker of Plasma Atherogenicity. *Dis. Markers* **2015**, *2015*, No. 591454.
(92) Zheng, S.; Han, T.; Xu, H.; Zhou, H.; Ren, X.; Wu, P.; Zheng, J.; Wang, L.; Zhang, M.; Jiang, Y.; Chen, Y.; Qiu, H.; Liu, W.; Hu, Y. Associations of Apolipoprotein B/apolipoprotein A-I Ratio with Pre-Diabetes and Diabetes Risks: A Cross-Sectional Study in Chinese Adults. *BMJ Open* **2017**, *7*, No. e014038.
(93) Fuertes-Martín, R.; Taverner, D.; Vallvé, J.-C.; Paredes, S.; Masana, L.; Correig Blanchar, X.; Amigó Grau, N. Characterization of 1H NMR Plasma Glycoproteins as a New Strategy To Identify Inflammatory Patterns in Rheumatoid Arthritis. *J. Proteome Res.* **2018**, *17*, 3730−3739.
(94) Wu, Q.; Zhou, L.; Sun, X.; Yan, Z.; Hu, C.; Wu, J.; Xu, L.; Li, X.; Liu, H.; Yin, P.; Li, K.; Zhao, J.; Li, Y.; Wang, X.; Li, Y.; Zhang, Q.; Xu, G.; Chen, H. Altered Lipid Metabolism in Recovered SARS Patients Twelve Years after Infection. *Sci. Rep.* **2017**, *7*, No. 9110.
(95) SARS. https://www.cdc.gov/sars/about/faq.html (accessed Mar 18 , 2021).

https://doi.org/10.1021/acs.jproteome.1c00224
J. Proteome Res. 2021, 20, 3315−3329